

An Efficient Catalytic Method for Hydrophosphination of Heterocumulenes with Diethylzinc as Precatalyst

Table of Contents

General Procedures.....	1
Syntheses of Zinc Compounds EtZnPPh₂ (A) and [{Ph₂PC(NⁱPr)₂ZnEt}₂ (C).....	2
Crystal Structural Data and Refinement Details for Compound C	7
General Catalytic Procedure for the Hydrophosphination of Heterocumulenes.....	8
Spectroscopic Data	9
References	28

General Procedures

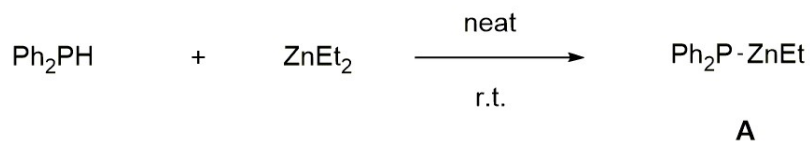
All manipulations were carried out under a purified nitrogen atmosphere using Schlenk techniques or inside a Mbraun MB 150-GI glove box. All solvents were refluxed over the appropriate drying agents and distilled prior to use. Commercially available chemicals were purchased from J&K chemical or Aldrich and used as received. No ³¹P-NMR-silent material was formed in all reactions, so we determined the catalytic yields by ³¹P NMR. ¹H, ¹³C, and ³¹P NMR spectra were recorded with a Varian Mercury Plus 400 MHz or Bruker Avance III 700 MHz spectrometer. Compounds

LAIH_2 ($\text{L} = \text{HC}(\text{CMeNAr})_2$, Ar = 2,6- $\text{Et}_2\text{C}_6\text{H}_3$) (**1**), and LZnEt (**2**) were prepared according to the literature procedures.^{[1][2]} Organophosphorus compounds **9i**, **9f**, **9j** and **9k** are new compounds. All other hydrophosphination products reported in this paper are known compounds which synthetic methods and catalytic reactions have been reported several times.^[3-9]

CCDC- 2097921 (**C**) contain the supplementary crystallographic data for this paper. This data can be obtained free of charge from The Cambridge Crystallographic Data Centre via www.ccdc.cam.ac.uk/data_request/cif.

Syntheses of Zinc Compounds EtZnPPh_2 (**A**) and $[\{\text{Ph}_2\text{PC}(\text{N}^i\text{Pr})_2\text{ZnEt}\}]_2$ (**C**)

Scheme S1. Synthesis of Zinc Compound EtZnPPh_2 (**A**)



Method for Preparation of EtZnPPh_2 (A**):** ZnEt_2 (1 M in hexane, 1 mL, 1 mmol) was added at room temperature to Ph_2PH (0.186 g, 1 mmol) under nitrogen atmosphere, and the reaction mixture was stirred for additional 12 h. The crude product was washed with hexane to afford white powder of **A** and dried in vacuo. (0.133 g, yield 67% based on Ph_2PH); m.p. >300 °C. It can be found that **A** is present in polymeric form from Figure S1, because , which is consistent with the conclusion of *J. G. Noltes*.^[10] ^1H NMR (400 MHz, CDCl_3 , ppm) δ 7.39 – 7.11 (m, 10H, Ar-*H*), 1.28 – 1.14 (d, J = 5.6 Hz, 3H, CH_3), 0.83 – 0.78 (d, J = 6.3 Hz, 2H, CH_2). ^{13}C NMR (176 MHz, CDCl_3 , ppm) δ 136.00, 135.03 – 132.86 (m), 129.54 – 126.79 (m), 24.45, 15.45. ^{31}P NMR (162 MHz, CDCl_3 , ppm) δ -14.95.

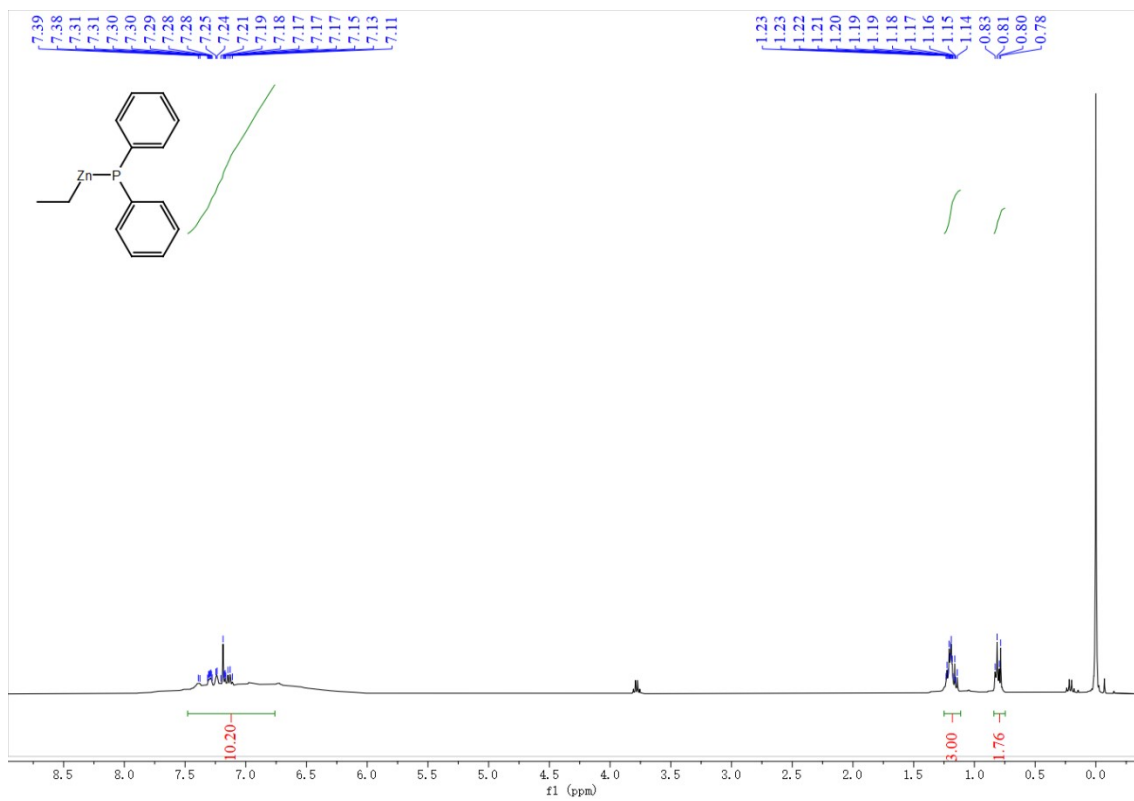


Figure S1. ^1H NMR spectrum (400 MHz, 298K, CDCl_3) of **A**

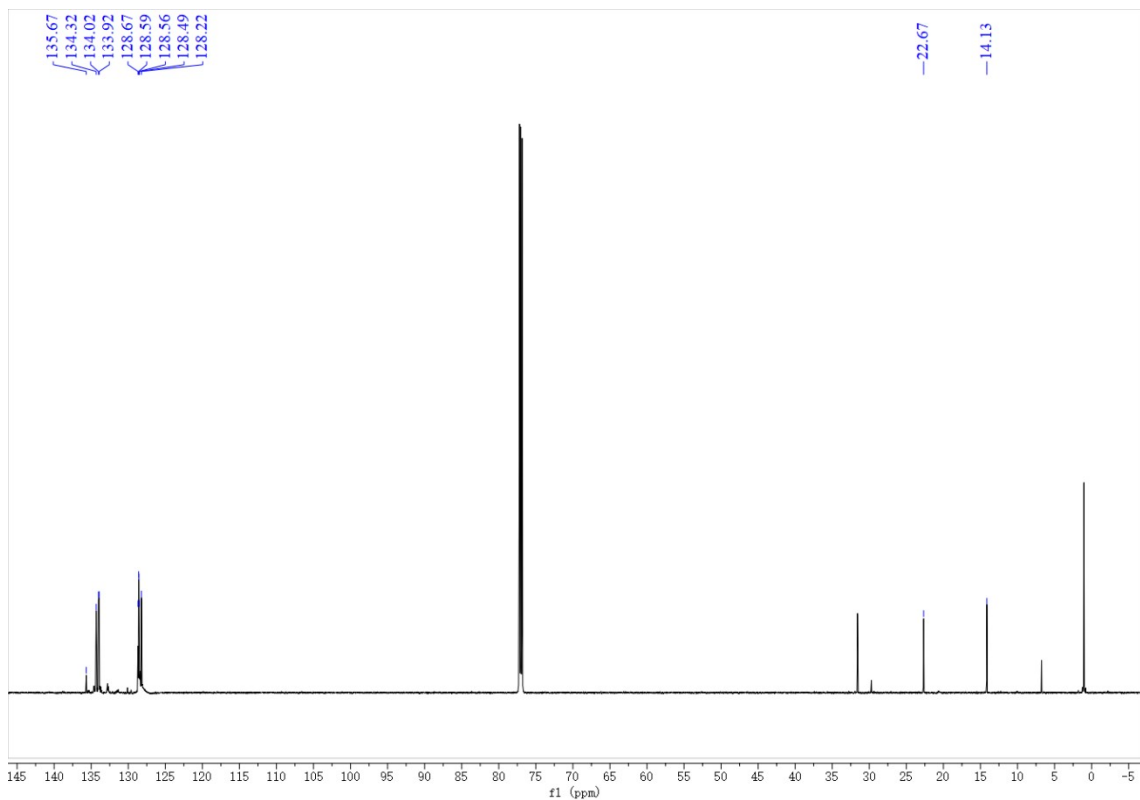


Figure S2. ^{13}C NMR spectrum (176 MHz, 298K, CDCl_3) of A

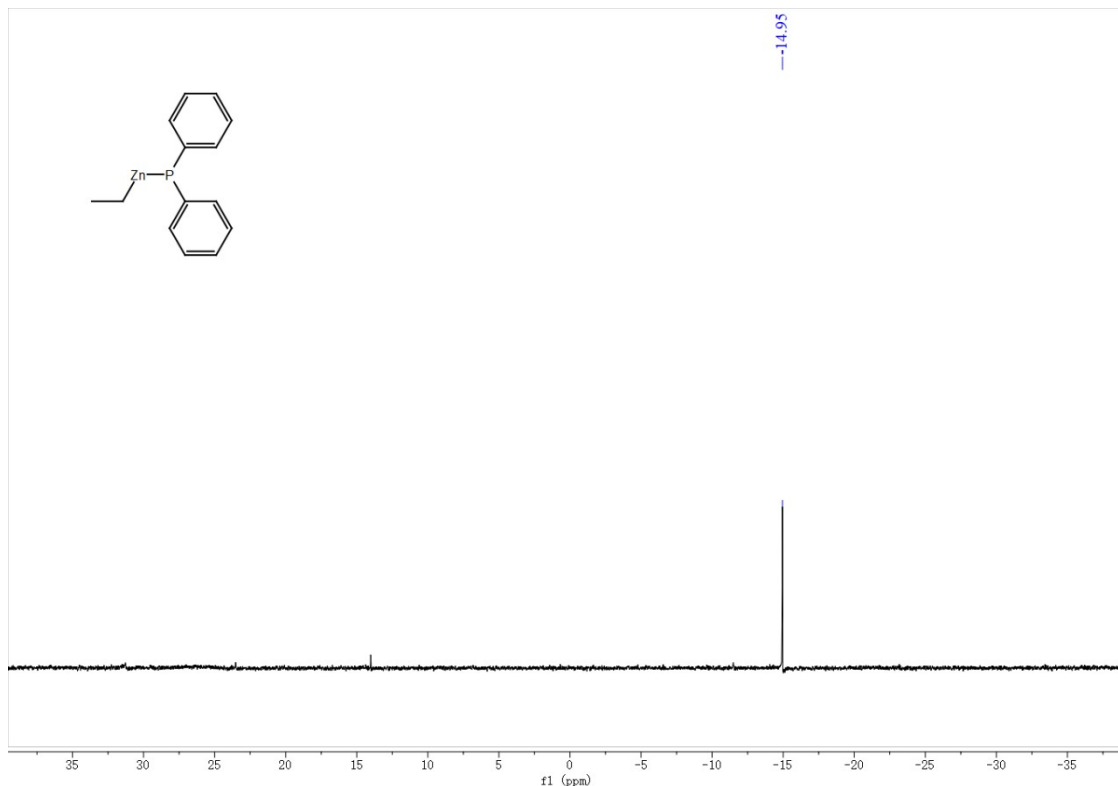
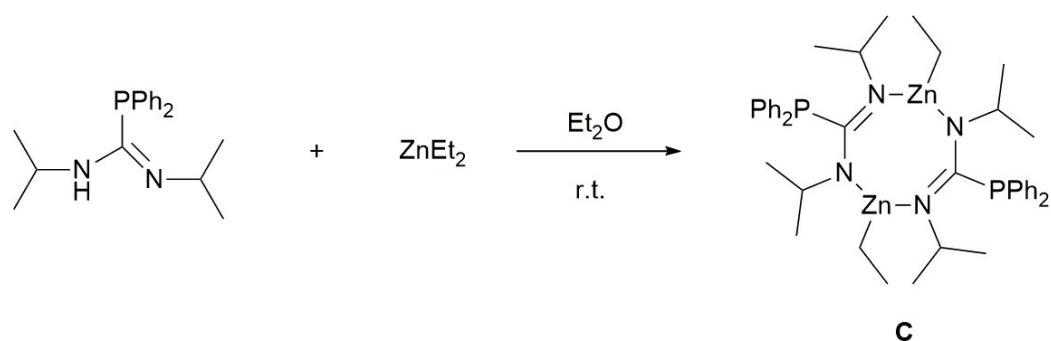


Figure S3. ^{31}P NMR spectrum (162 MHz, 298K, CDCl_3) of A

Scheme S2. Synthesis of Zinc Compound $[\{\text{Ph}_2\text{PC}(\text{N}^i\text{Pr})_2\}\text{ZnEt}]_2$ (**C**)



Method for Preparation of $[\{\text{Ph}_2\text{PC}(\text{N}^i\text{Pr})_2\}\text{ZnEt}]_2$ (C**):** ZnEt_2 (1 M in hexane, 1 mL, 1 mmol)

was added at room temperature to a solution of $^i\text{PrN}=\text{C}(\text{PPh}_2)(\text{NH}^i\text{Pr})$ (**9a**) (0.311 g, 1 mmol) in

Et_2O (5 mL) under nitrogen atmosphere, and the reaction mixture was stirred for additional 12 h,

stored overnight at -32 °C. The crude product was crystallized from toluene to afford colorless crystals of **C** and dried in vacuo. (0.63 g, yield 59% based on *i*PrN=C(PPh₂)(NH*i*Pr) (**9a**)); m.p. 97~102 °C.¹H NMR (400 MHz, CDCl₃, ppm) δ 7.73 – 7.63 (m, 2H, NH), 7.52 – 6.91 (m, 20H, Ar-H), 3.57 – 3.41 (hept, *J* = 6.4 Hz, 4H, CH(CH₃)₂), 1.19 – 1.11 (d, *J* = 6.4 Hz, 30H, CH₃), 0.91 – 0.89 (d, *J* = 4.3 Hz, 4H, CH₂);¹³C NMR (176 MHz, CDCl₃, ppm) δ 157.47, 139.46 – 130.92 (d, *J* = 19.5 Hz), 131.85, 54.06 – 50.71 (d, *J* = 36.1 Hz), 50.43, 44.59, 28.72 – 20.54 (d, *J* = 20.8 Hz), 23.24, 8.65, 4.38.³¹P NMR (162 MHz, CDCl₃, ppm) δ -17.70. **Anal Calcd** for C₄₂H₅₈N₄P₂Zn₂: C, 62.15; H, 7.20; N, 6.90. Found, C, 54.58; H, 6.095; N, 6.31.

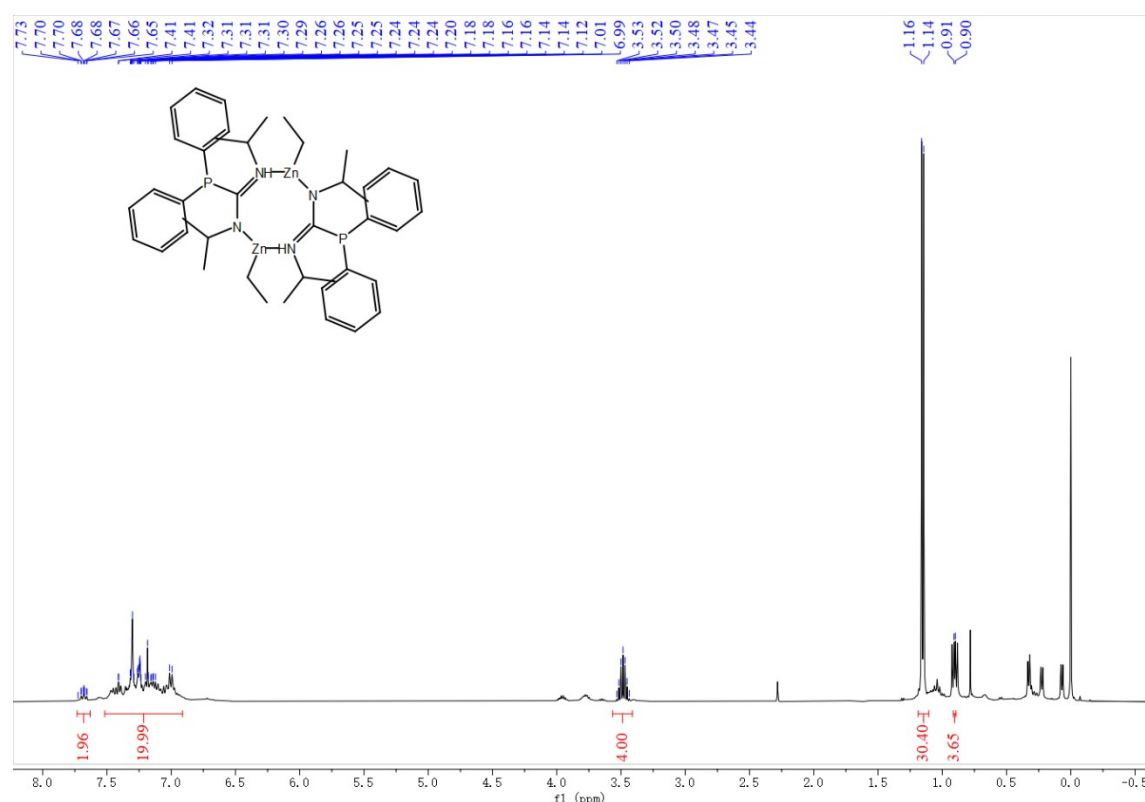


Figure S4. ¹H NMR spectrum (400 MHz, 298K, CDCl₃) of **C**

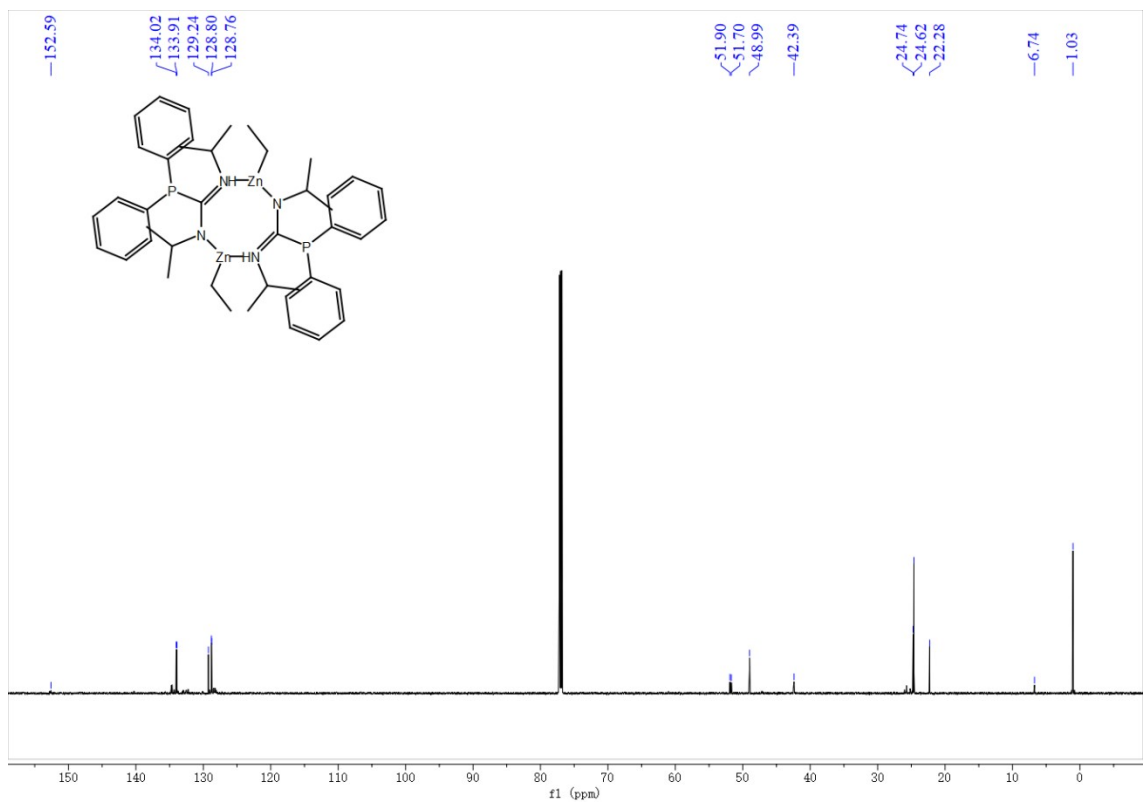


Figure S5. ^{13}C NMR spectrum (176 MHz, 298K, CDCl_3) of **C**

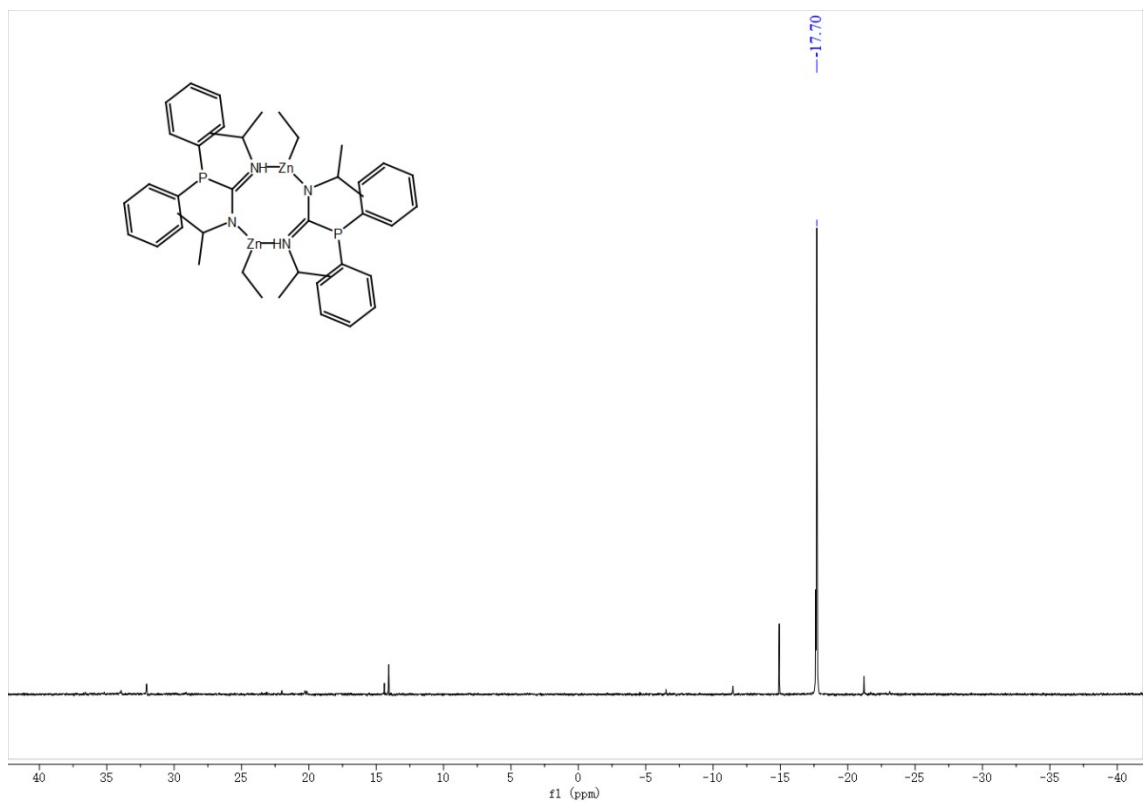


Figure S6. ^{31}P NMR spectrum (162 MHz, 298K, CDCl_3) of **C**

Crystal Structural Data and Refinement Details for Compound C

The single crystal of **C** was mounted with glue on a glass fiber and crystal data were collected on the Rigaku AFC10 Saturn724 + (2×2 bin mode) diffractometer equipped with graphite-monochromated Mo K α radiation ($\lambda = 0.71073 \text{ \AA}$). Empirical absorption correction was applied using the SADABS program.^[11] The structure was solved by the SHELXT-2014 program^[12] and refined by full-matrix least squares on F2 using the SHELXL-2016 program.^[13] The summary of the crystal data are given in Table S1.

Table S1: Single crystal X-ray structural data and refinement details for compound **C**.

Compound	C
CCDC	2097921
Empirical formula	$\text{C}_{42}\text{H}_{58}\text{N}_4\text{P}_2\text{Zn}_2$
Formula weight	811.60
Temperature (K)	296.15
Crystal system	triclinic
Space group	P-1
a (\AA)	8.4939(4)
b (\AA)	14.3347(7)
c (\AA)	18.6216(9)
α ($^\circ$)	101.438(2)

β (°)	98.239(2)
γ (°)	106.0400(10)
Volume (Å ³)	2088.01(18)
Z	2
ρ_{calc} (g/cm ³)	1.291
μ (mm ⁻¹)	1.258
Crystal size (mm)	0.2 × 0.15 × 0.1
Θ range (deg)	2.282 - 49.998
Reflections collected	20416
R(int)	0.0662
Data/restraints/parameter	7329/0/451
s	
F (000)	856.0
R1 ^a , wR2 ^b ($I > 2\sigma(I)$)	0.0271, 0.0669
R1 ^a , wR2 ^b (all data)	0.0340, 0.0689

General Catalytic Procedure for the Hydrophosphination of Heterocumulenes

All reactions were carried out under nitrogen atmosphere. Catalyst **8** (5 mol%), heterocumulene (1 mmol) and Ph₂PH (0.186g, 1 mmol) were sealed in a 10 mL Schlenk flask equipped with a magnetic stir bar inside the glove box. The reaction mixture was stirred at room temperature for

0.1 - 24 hours depending on the nature of the starting material. The progress of the reaction was monitored by ^1H and ^{31}P NMR spectroscopy using anisole (10 mol%) as an internal standard.

Spectroscopic Data

$^1\text{PrN}=\text{C}(\text{PPh}_2)(\text{NHPr})$ (**9a**)

White solid (99% yield). ^1H NMR (400 MHz, CDCl_3 , ppm) δ 7.38 – 7.26 (m, 10H, Ar-H), 4.05 – 3.88 (m, 2H, $\text{CH}(\text{CH}_3)_2$), 3.44 – 3.36 (d, J = 7.2 Hz, 1H, NH), 0.96 – 0.83 (dd, J = 10.7, 6.3 Hz, 12H, $\text{CH}(\text{CH}_3)_2$). ^{13}C NMR (101 MHz, CDCl_3) δ 151.83 (d, J = 30.8 Hz), 133.93 (d, J = 13.4 Hz), 133.32 (d, J = 19.6 Hz), 128.61, 128.09 (d, J = 6.9 Hz), 52.06 (d, J = 35.8 Hz), 42.79, 24.32, 21.71.

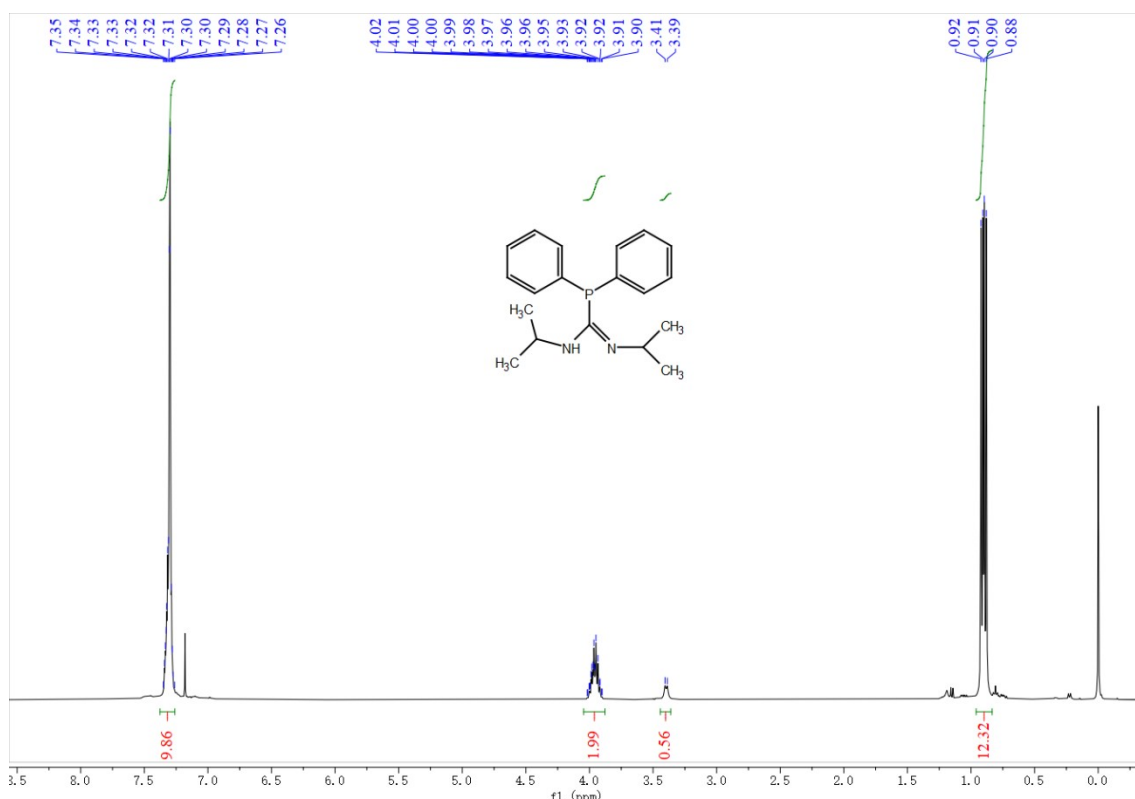


Figure S7. ^1H NMR spectrum (400 MHz, 298K, CDCl_3) of **9a**

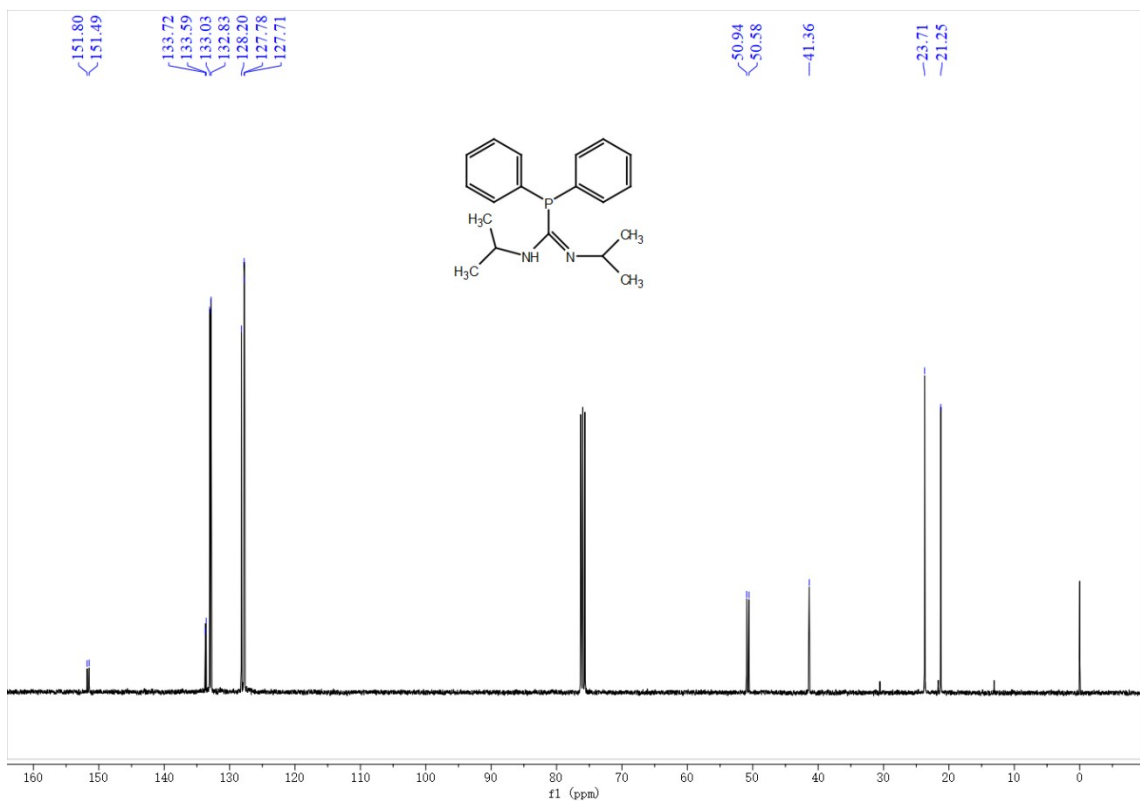


Figure S8. ^{13}C NMR spectrum (101 MHz, 298K, CDCl_3) of **9a**

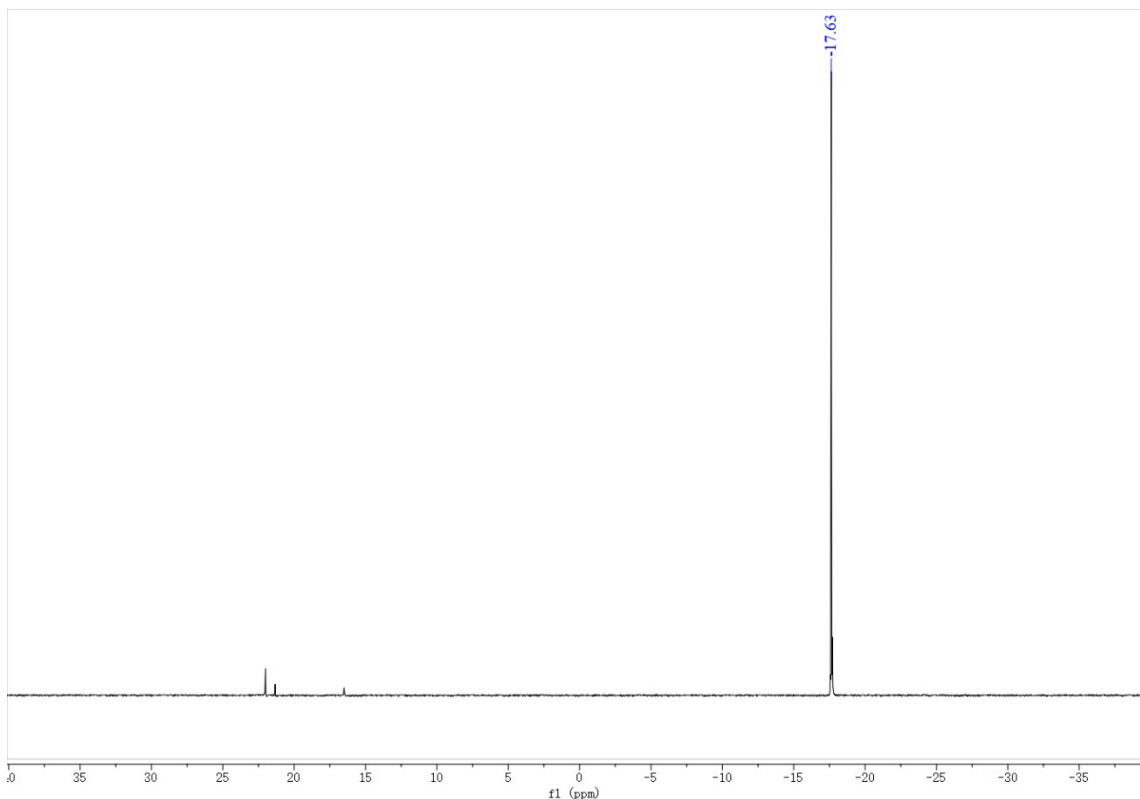


Figure S9. ^{31}P NMR spectrum (101 MHz, 298K, CDCl_3) of **9a**

*CyN=C(PPh₂)(NHCy) (**9b**)*

White solid (99% yield). ¹H NMR (400 MHz, CDCl₃, ppm) δ 7.38 – 7.26 (m, 10H, Ar-H), 3.84 – 3.66 (m, 1H, CH), 3.62 – 3.46 (m, 1H, CH), 1.83 – 0.72 (m, 20H, Cy). ¹³C NMR (101 MHz, CDCl₃, ppm) δ 152.14 (d, *J* = 30.7 Hz), 128.35, 127.85 (d, *J* = 6.9 Hz), 59.23 (d, *J* = 34.3 Hz), 47.52, 34.38, 31.98, 25.01 (d, *J* = 12.8 Hz), 24.23, 23.18. ³¹P NMR (162 MHz, CDCl₃, ppm) δ -18.52.

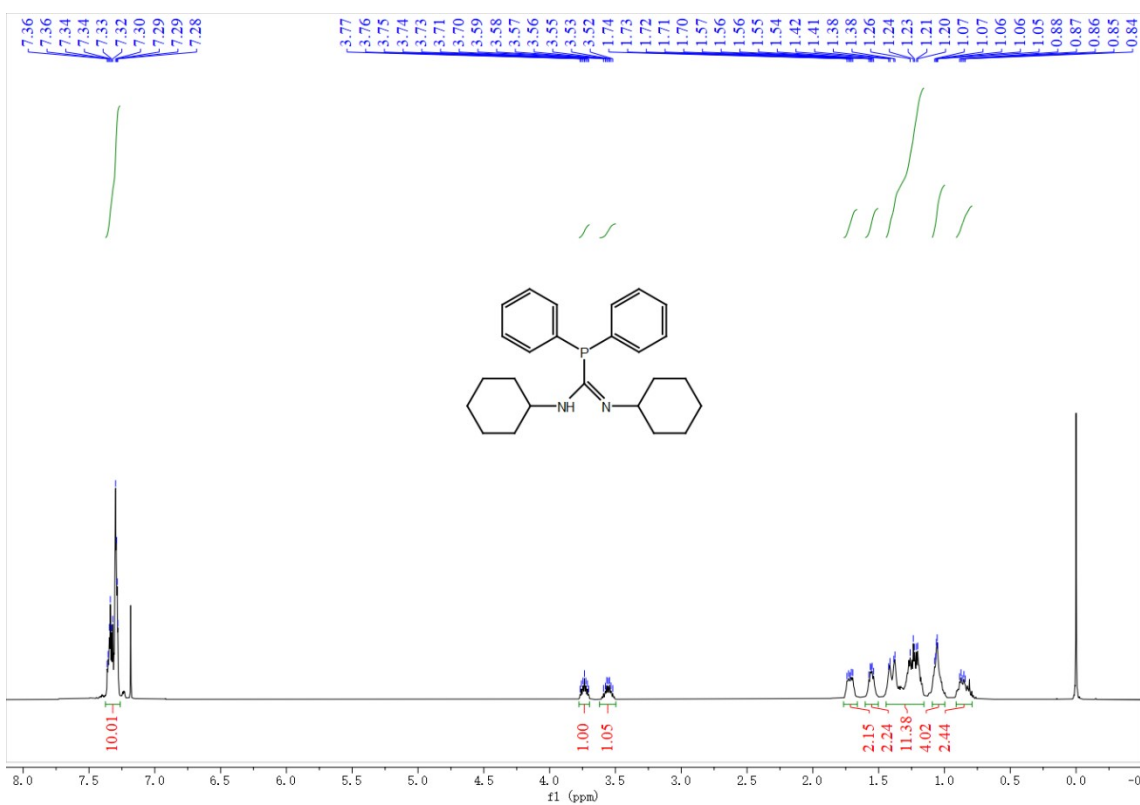


Figure S10. ¹H NMR spectrum (400 MHz, 298K, CDCl₃) of **9b**

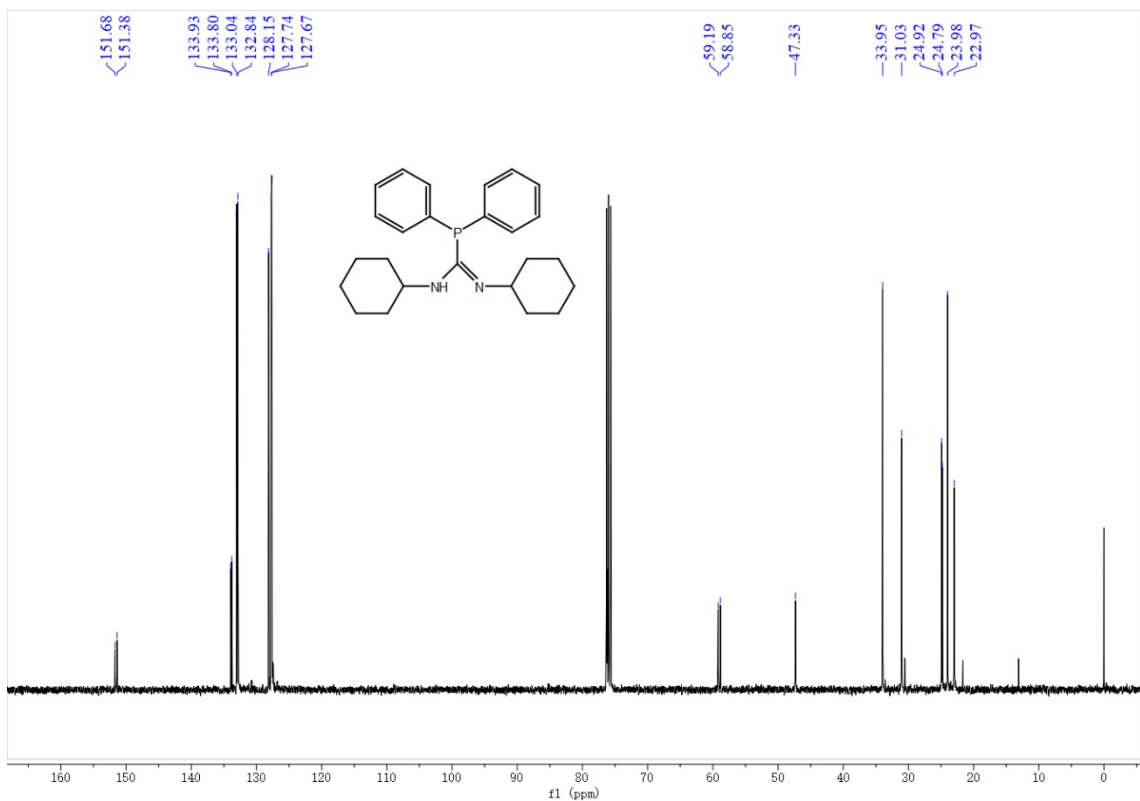


Figure S11. ^{13}C NMR spectrum (101 MHz, 298K, CDCl_3) of **9b**

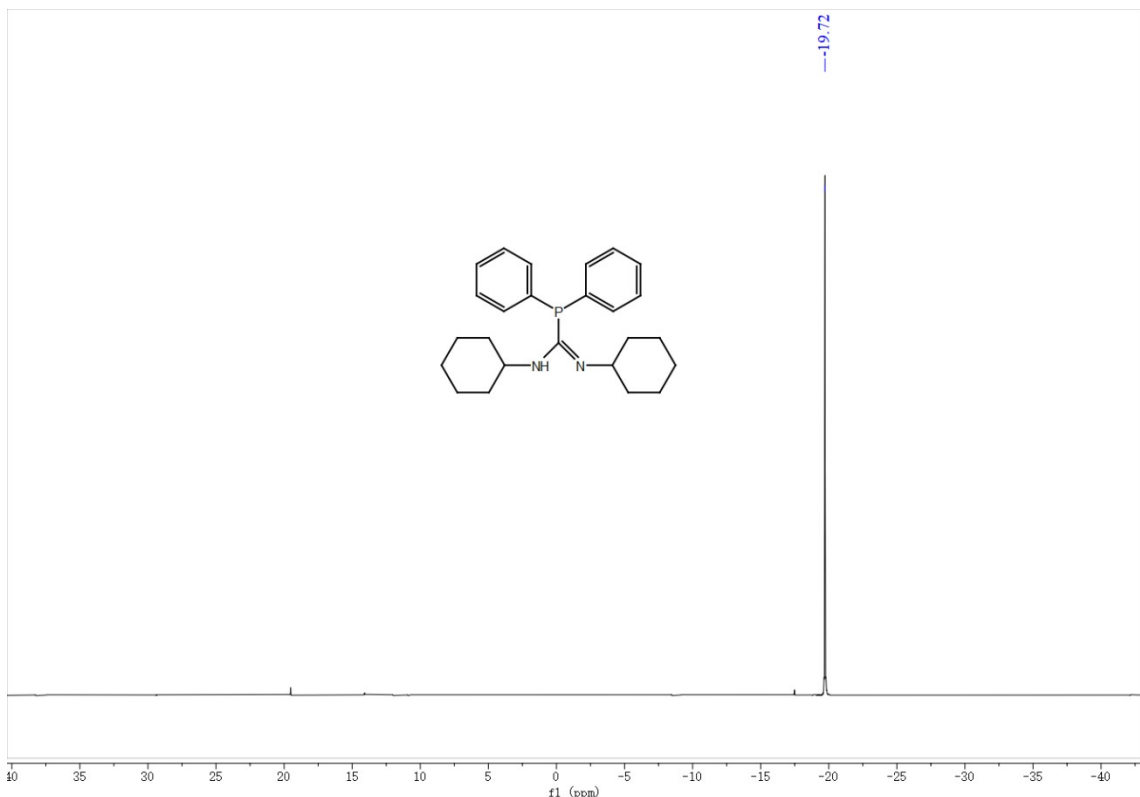


Figure S12. ^{31}P NMR spectrum (162 MHz, 298K, CDCl_3) of **9b**

Ph₂PC(O)NH(*i*Pr) (**9c**)

White solid (99% yield). ^1H NMR (400 MHz, CDCl_3 , ppm) δ 7.47 – 7.40 (m, 4H, Ar-*H*), 7.37 – 7.26 (m, 6H, Ar-*H*), 5.47 – 5.33 (d, J = 9.1 Hz, 1H, NH), 4.17 – 4.04 (m, 1H, $\text{CH}(\text{CH}_3)_2$), 1.02 – 0.94 (d, J = 6.6 Hz, 6H, $\text{CH}(\text{CH}_3)_2$). ^{13}C NMR (101 MHz, CDCl_3) δ 181.24 – 171.19 (d, J = 13.0 Hz), 139.09 – 131.37 (m), 131.58 – 121.53 (m), 44.54, 26.00. ^{31}P NMR (162 MHz, CDCl_3 , ppm) δ -3.8.

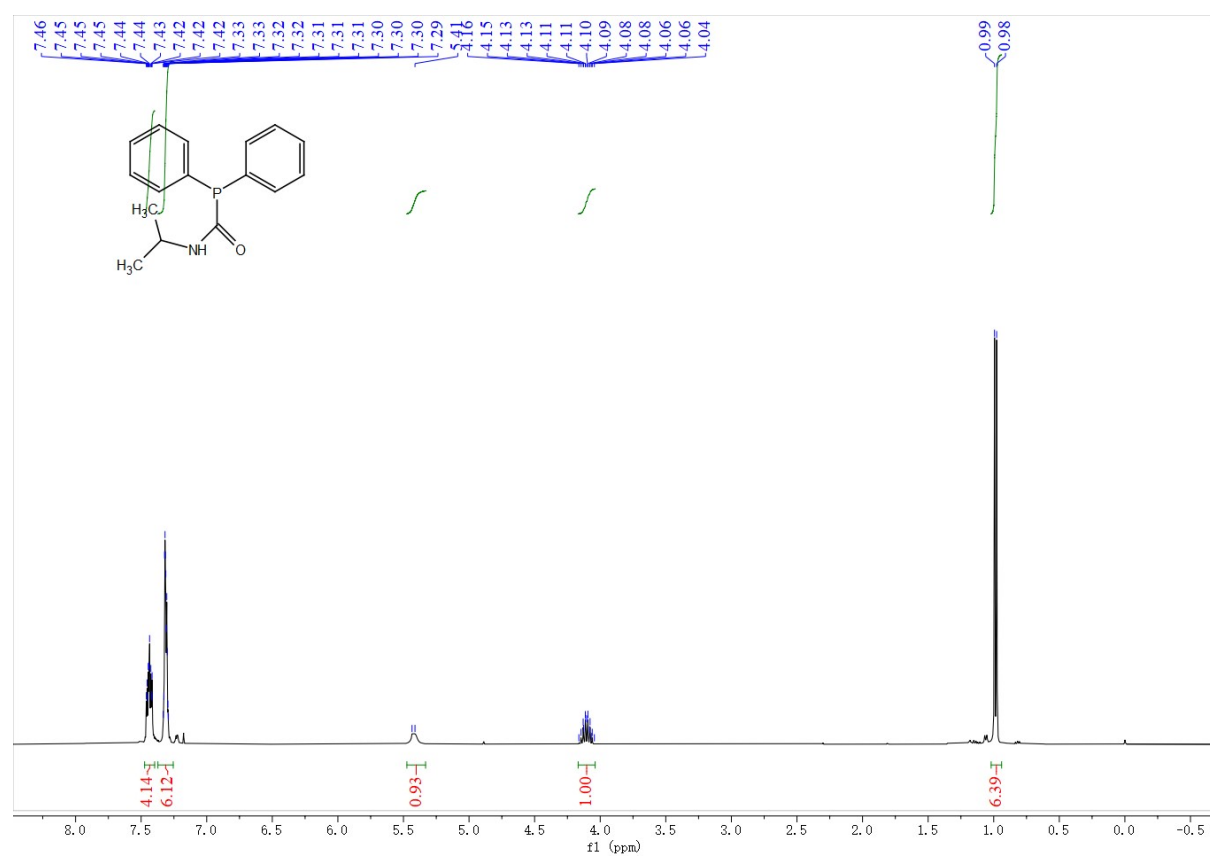


Figure S13. ^1H NMR spectrum (400 MHz, 298K, CDCl_3) of **9c**

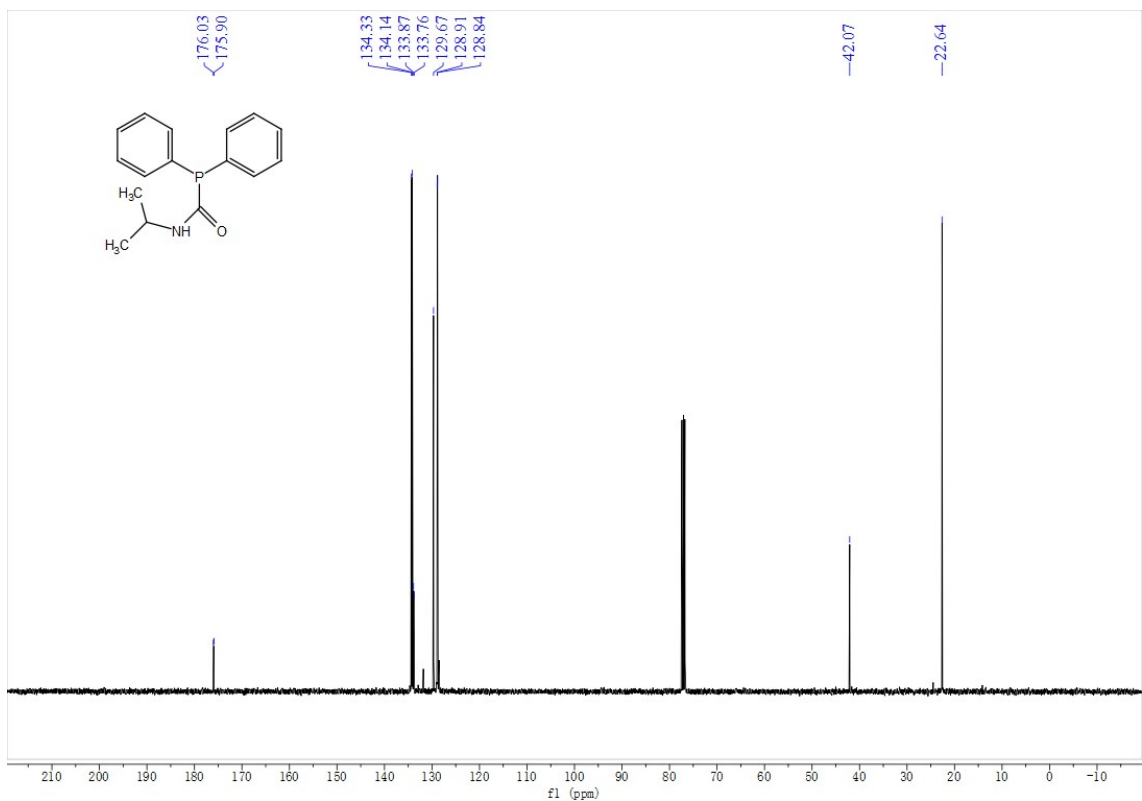


Figure S14. ^{13}C NMR spectrum (101 MHz, 298K, CDCl_3) of **9c**

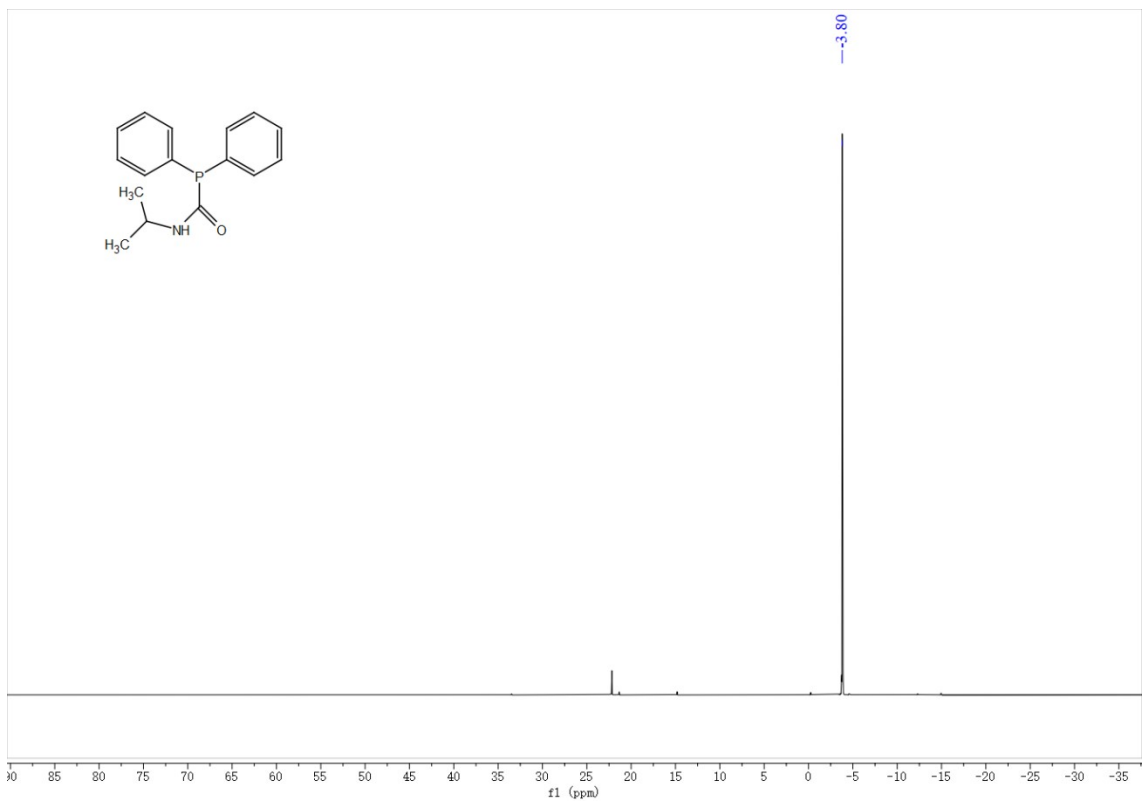


Figure S15. ^{31}P NMR spectrum (162 MHz, 298K, CDCl_3) of **9c**

$\text{Ph}_2\text{PC(O)NHCy}$ (**9d**)

White solid (99% yield). ^1H NMR (400 MHz, CDCl_3 , ppm) δ 7.52 – 7.39 (m, 4H, Ar-H), 7.35 – 7.28 (m, 6H, Ar-H), 5.56 – 5.44 (d, J = 8.2 Hz, 1H, NH), 3.90 – 3.76 (m, 1H, CH), 1.87 – 1.66 (m, 2H, CH_2), 1.57 – 1.36 (m, 3H, CH_2), 1.35 – 1.16 (m, 2H, CH_2), 1.13 – 0.87 (m, 3H, CH_2). ^{13}C NMR (176 MHz, CDCl_3 , ppm) δ 175.86 – 175.77 (d, J = 3.7 Hz), 134.41 – 134.09 (d, J = 19.0 Hz), 131.07 – 123.45 (d), 59.47 – 44.74 (d, J = 21.9 Hz), 37.12 – 31.71 (d, J = 5.3 Hz), 27.87 – 15.56 (d, J = 164.3 Hz). ^{31}P NMR (162 MHz, CDCl_3 , ppm) δ -4.10.

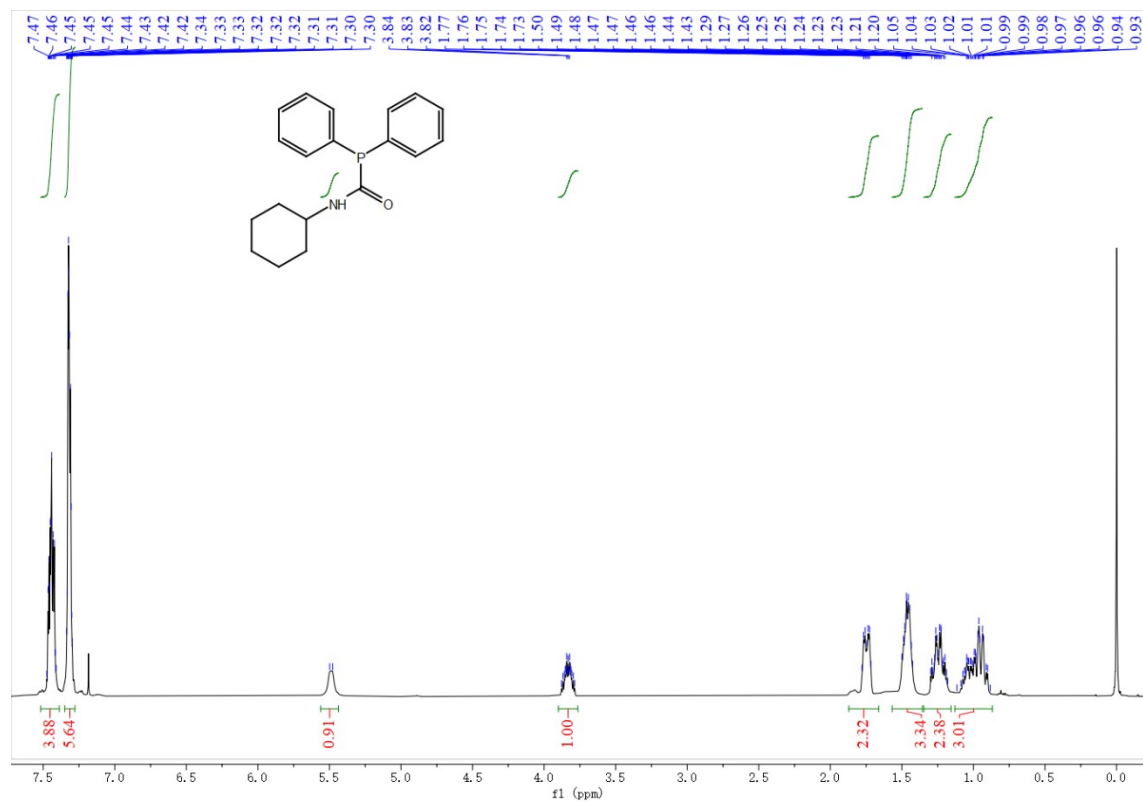


Figure S16. ^1H NMR spectrum (400 MHz, 298K, CDCl_3) of **9d**

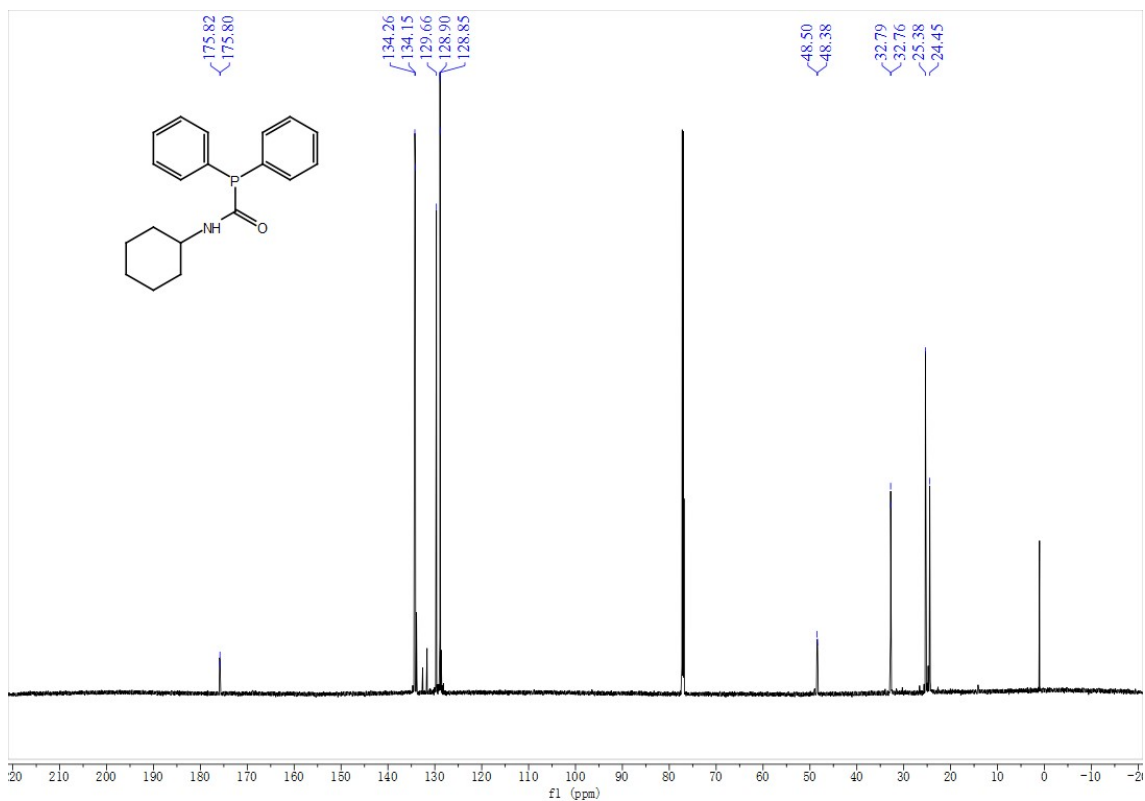


Figure S17. ^{13}C NMR spectrum (101 MHz, 298K, CDCl_3) of **9d**

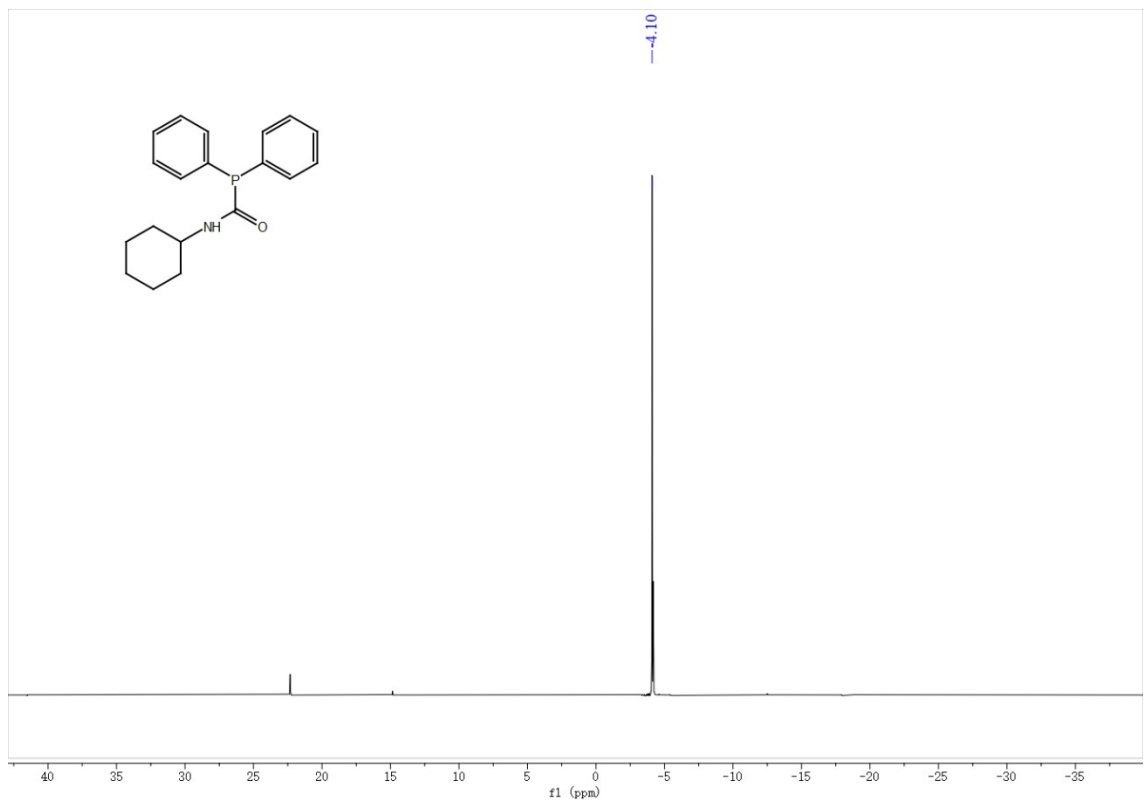


Figure S18. ^{31}P NMR spectrum (162 MHz, 298K, CDCl_3) of **9d**

$\text{Ph}_2\text{PC(O)NH('Bu)}$ (**9e**)

White solid (44% yield). ^1H NMR (400 MHz, CDCl_3 , ppm) δ 7.51 – 7.37 (m, 4H, Ar-H), 7.37 – 7.26 (m, 6H, Ar-H), 5.52 – 5.36 (s, 1H, NH), 1.47 – 1.02 (s, 9H, 'Bu). ^{13}C NMR (101 MHz, CDCl_3 , ppm) δ 175.24 – 174.73, 133.31 – 133.19, 133.12 – 133.00 (d, $J = 7.1$ Hz), 129.13, 128.03 – 127.28 (d, $J = 7.3$ Hz), 56.36 – 48.85 (d, $J = 2.3$ Hz), 33.67. ^{31}P NMR (162 MHz, CDCl_3 , ppm) δ -2.08.

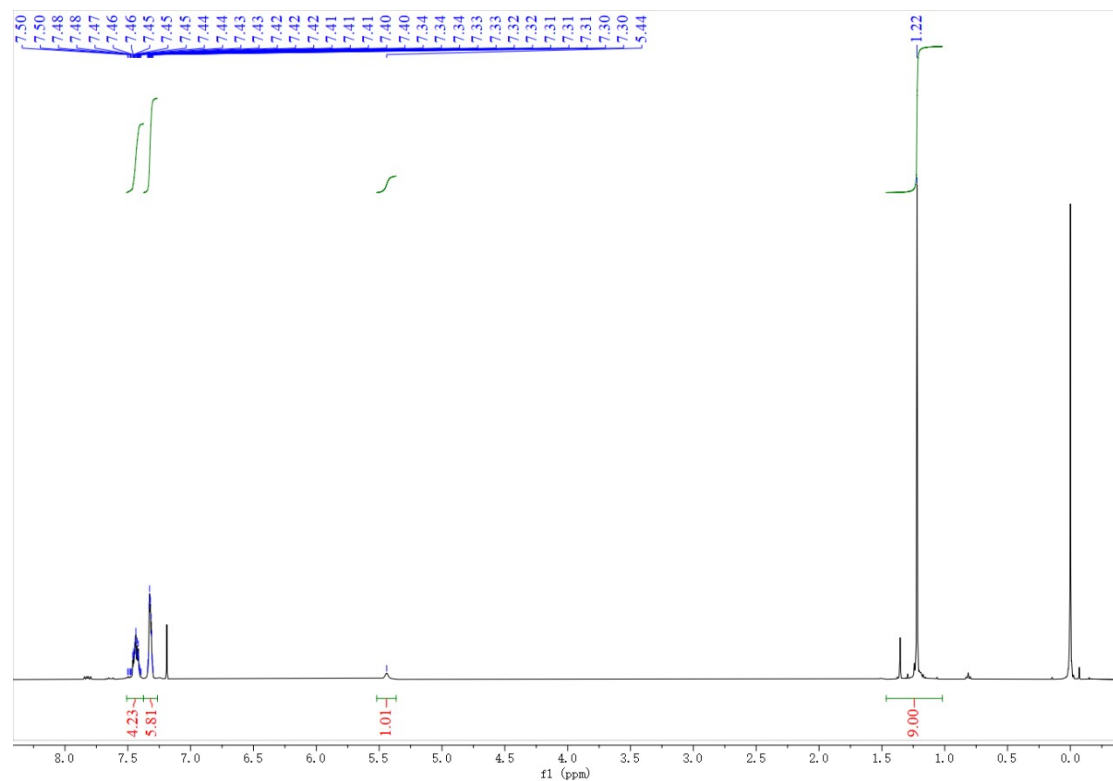


Figure S19. ^1H NMR spectrum (400 MHz, 298K, CDCl_3) of **9e**

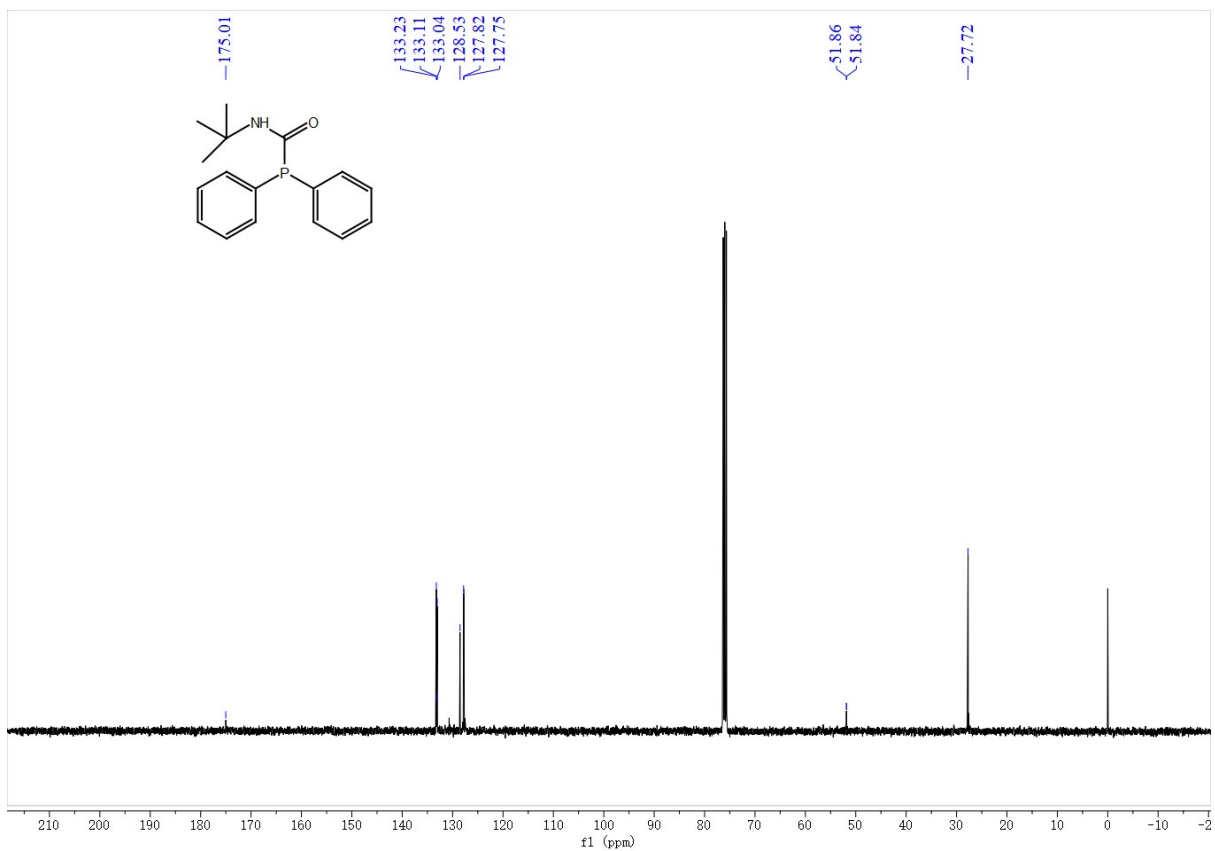


Figure S20. ^{13}C NMR spectrum (101 MHz, 298K, CDCl_3) of **9e**

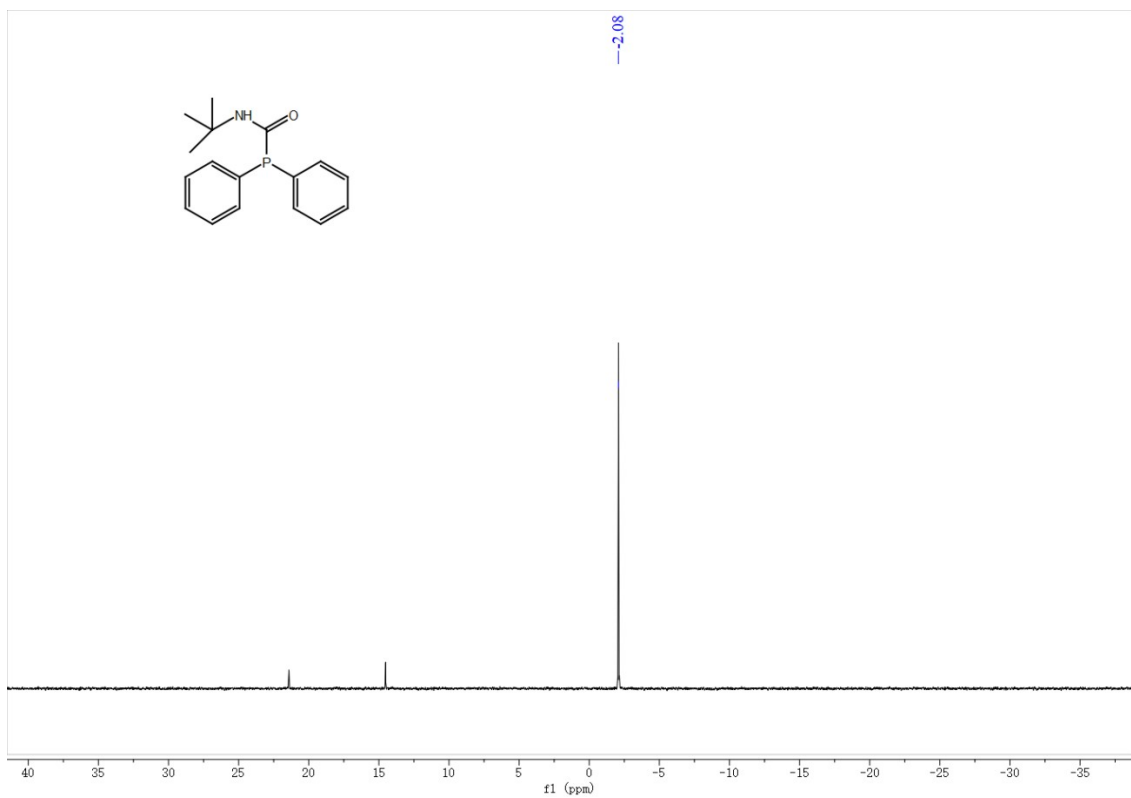


Figure S21. ^{31}P NMR spectrum (162 MHz, 298K, CDCl_3) of **9e**

$\text{Ph}_2\text{PC(S)NH}(\text{iPr})$ (**9f**)

Green solid (98% yield). ^1H NMR (400 MHz, CDCl_3 , ppm) δ 7.46 – 7.29 (m, 10H, Ar-H), 7.04 – 6.91 (s, 1H, NH), 4.75 – 4.62 (m, 1H, $\text{CH}(\text{CH}_3)_2$), 1.10 – 1.04 (d, $J = 6.5$ Hz, 6H, $\text{CH}(\text{CH}_3)_2$). ^{13}C NMR (101 MHz, CDCl_3 , ppm) δ 206.70 – 205.64 (d, $J = 38.2$ Hz), 134.76 – 133.76 (m), 130.24 – 129.78, 129.47 – 128.72 (d, $J = 7.4$ Hz), 56.90 – 38.43 (d, $J = 1.7$ Hz), 27.89. ^{31}P NMR (162 MHz, CDCl_3 , ppm) δ -14.38.

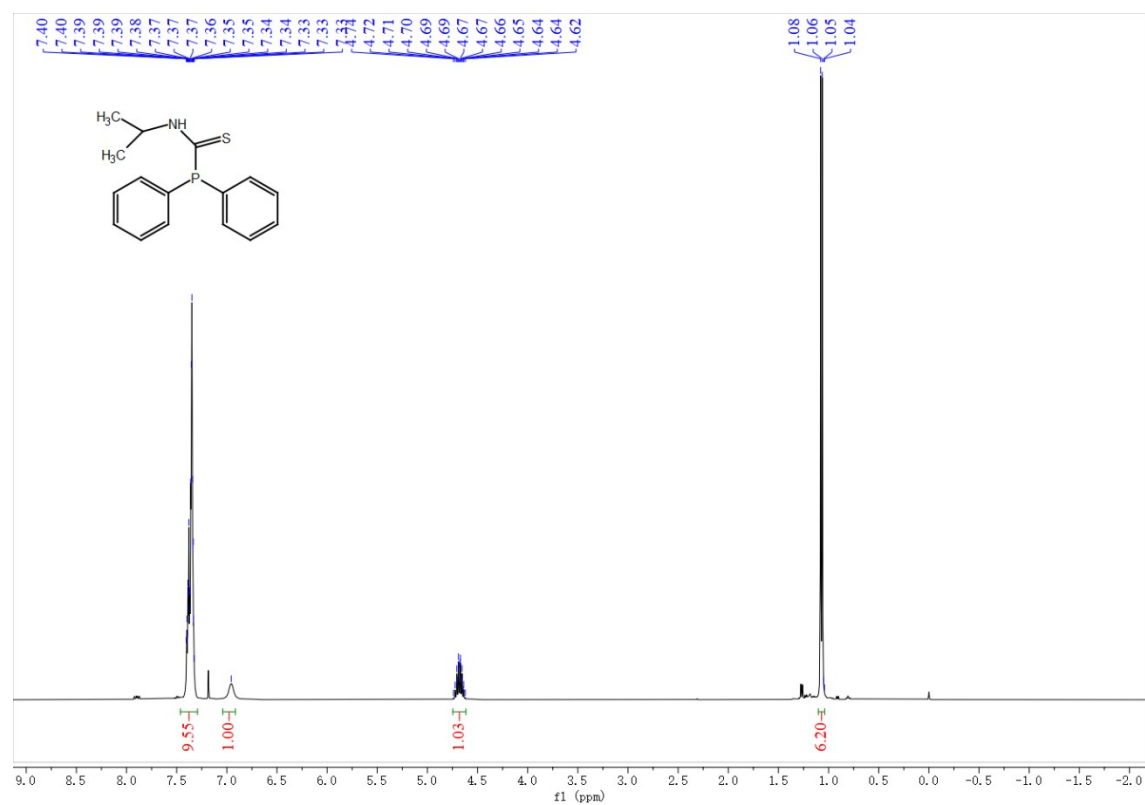


Figure S22. ^1H NMR spectrum (400 MHz, 298K, CDCl_3) of **9f**

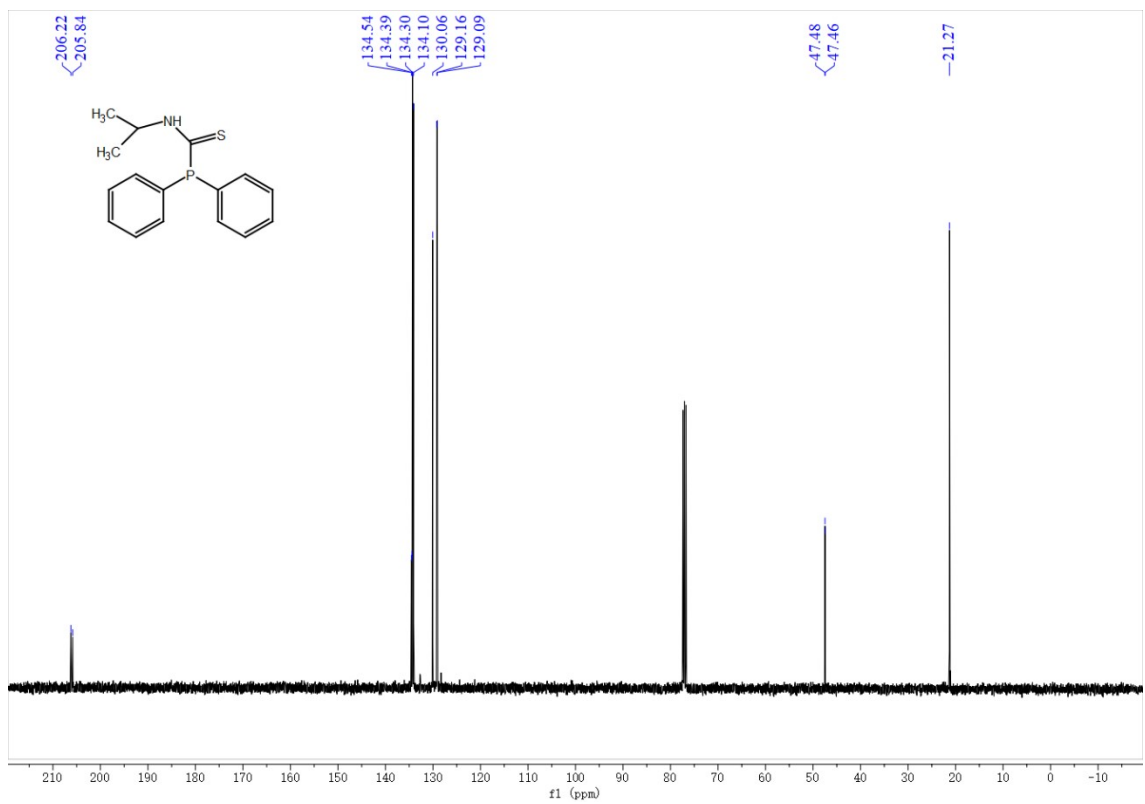


Figure S23. ^{13}C NMR spectrum (101 MHz, 298K, CDCl_3) of **9f**

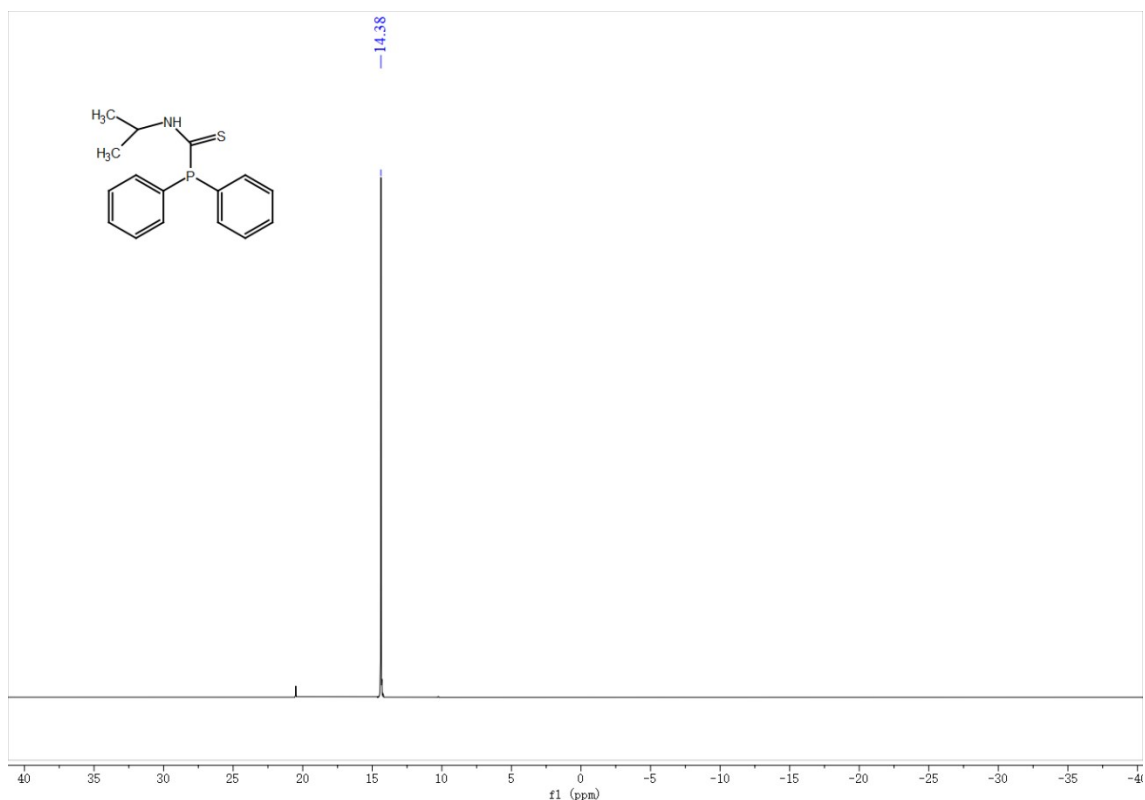


Figure S24. ^{31}P NMR spectrum (162 MHz, 298K, CDCl_3) of **9f**

$\text{Ph}_2\text{PC(S)NH}_2$ (**9g**)

Green solid (97% yield). ^1H NMR (400 MHz, CDCl_3 , ppm) δ 7.43 – 7.32 (m, 10H, Ar-H), 7.12 – 7.04 (m, 1H,

NH), 4.52 – 4.39 (m, 1H, CH), 1.89 – 1.81 (m, 2H, CH_2), 1.52 – 1.23 (m, 5H, CH_2), 1.16 – 0.99 (m, 3H, CH_2).

^{13}C NMR (101 MHz, CDCl_3 , ppm) δ 208.02 – 199.87 (d, $J = 38.0$ Hz), 138.05 – 130.33 (d, $J = 20.4$ Hz), 129.68

– 128.62, 128.53 – 127.29 (d, $J = 7.3$ Hz), 54.40, 31.63, 25.09, 23.48. ^{31}P NMR (162 MHz, CDCl_3 , ppm) δ -

14.01.

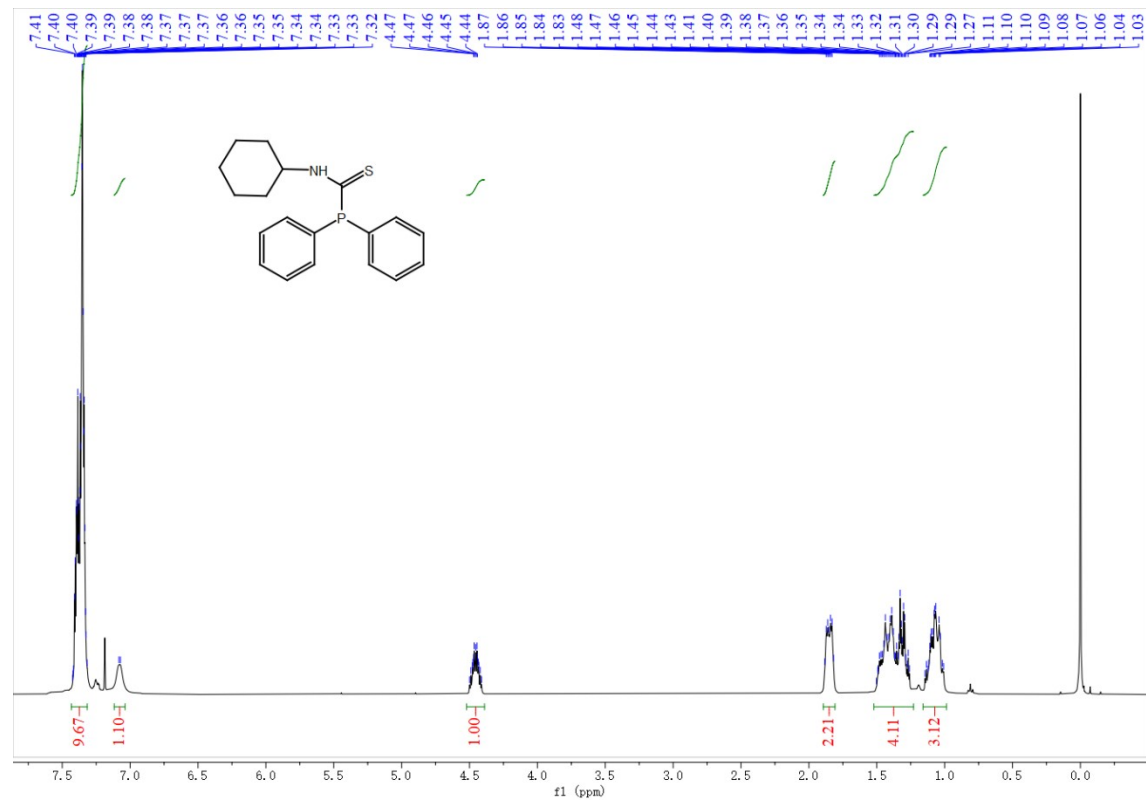


Figure S25. ^1H NMR spectrum (400 MHz, 298K, CDCl_3) of **9g**

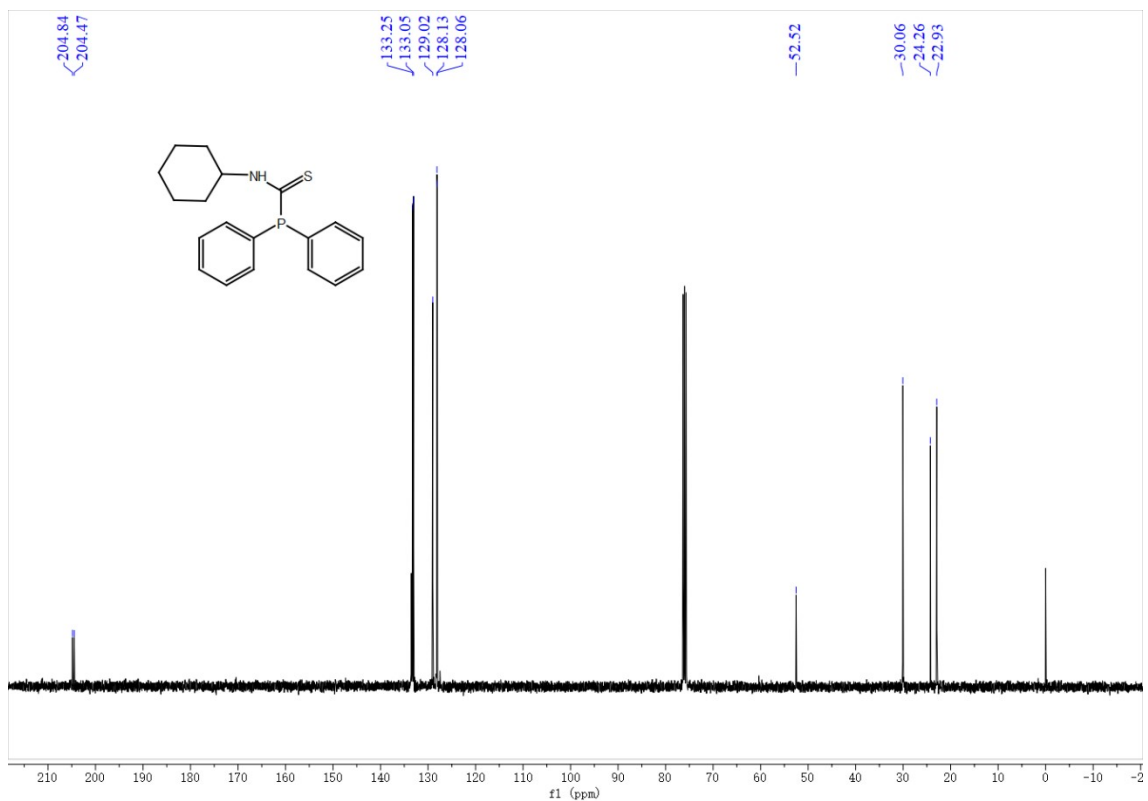


Figure S26. ^{13}C NMR spectrum (101 MHz, 298K, CDCl_3) of **9g**



Figure S27. ^{31}P NMR spectrum (162 MHz, 298K, CDCl_3) of **9g**

$\text{Ph}_2\text{PC(S)NH}({}^t\text{Bu})$ (**9h**)

Green solid (62% yield). ^1H NMR (400 MHz, CDCl_3 , ppm) δ 7.43 – 7.30 (m, 10H, Ar-H), 7.02 – 6.97 (s, 1H, NH), 1.43 – 1.31 (s, 9H, ${}^t\text{Bu}$). ^{13}C NMR (101 MHz, CDCl_3 , ppm) δ 205.79 – 204.63 (d, $J = 39.8$ Hz), 135.11 – 133.60 (d, $J = 17.3$ Hz), 133.48 – 132.31 (d, $J = 20.2$ Hz), 129.36, 128.38 – 127.70 (d, $J = 7.1$ Hz), 57.99, 28.71 – 22.54 (d, $J = 1.4$ Hz). ^{31}P NMR (162 MHz, CDCl_3 , ppm) δ -17.17.

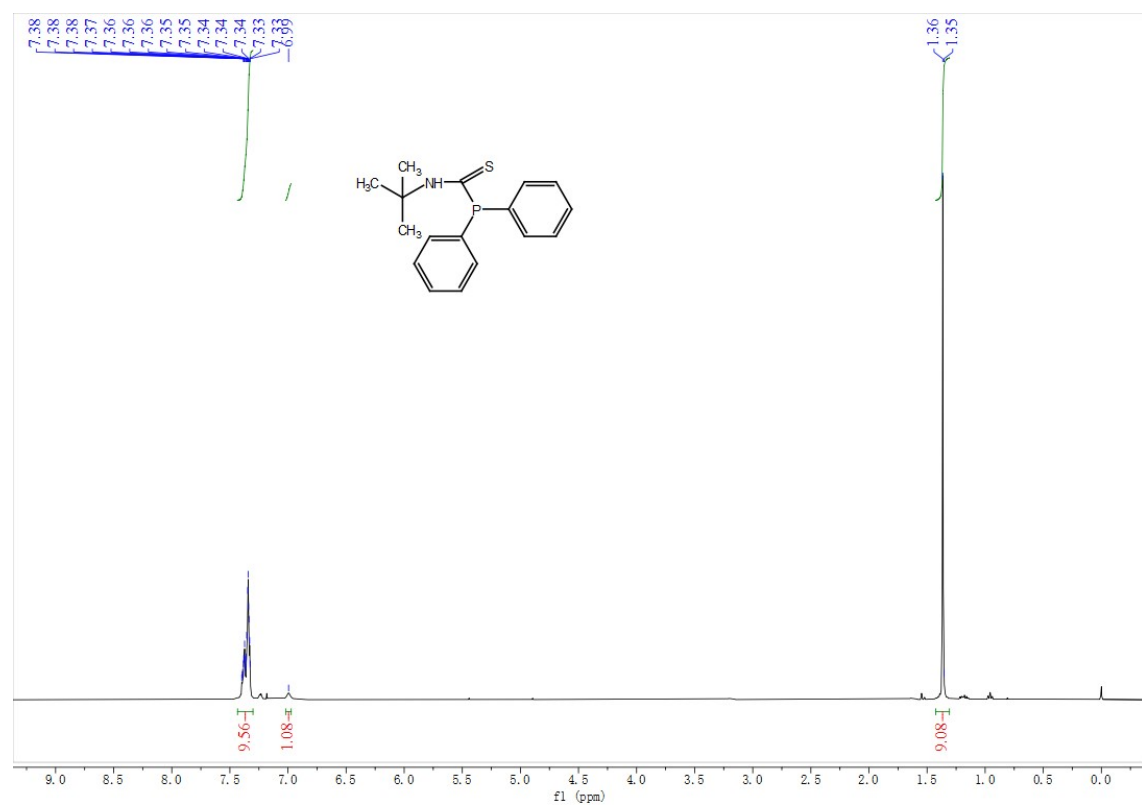


Figure S28. ^1H NMR spectrum (400 MHz, 298K, CDCl_3) of **9h**

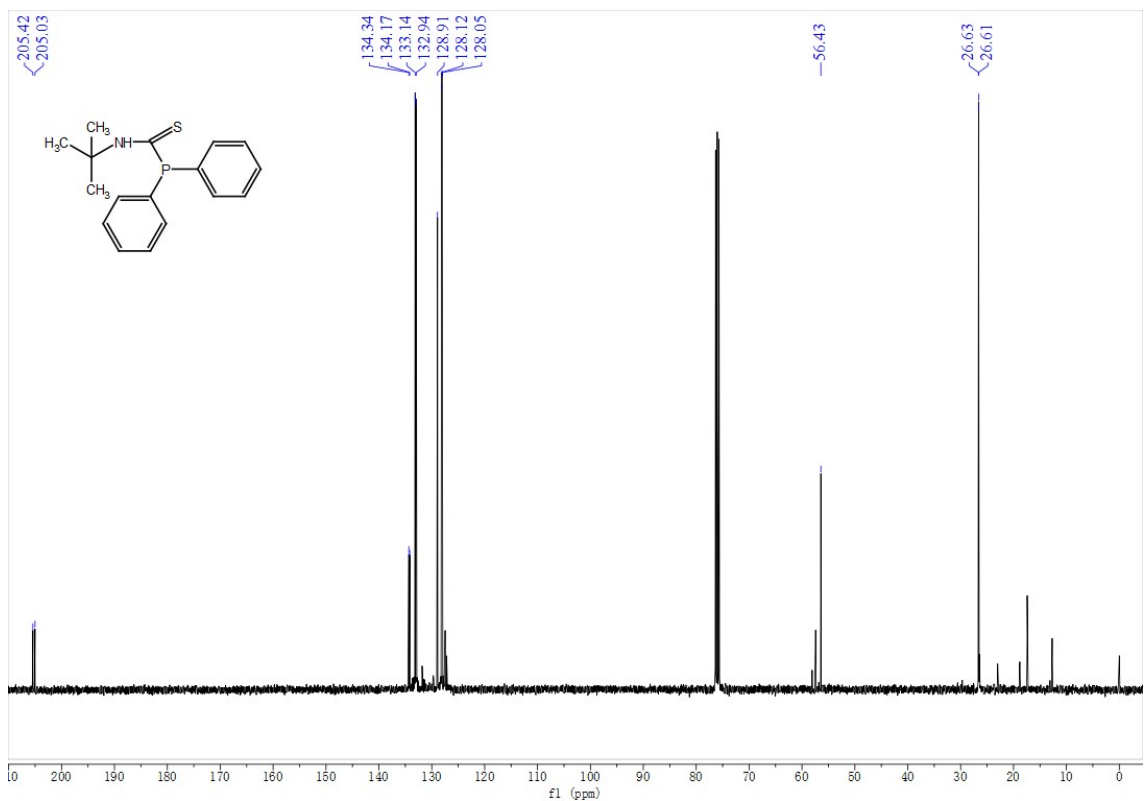


Figure S29. ^{13}C NMR spectrum (101 MHz, 298K, CDCl_3) of **9h**

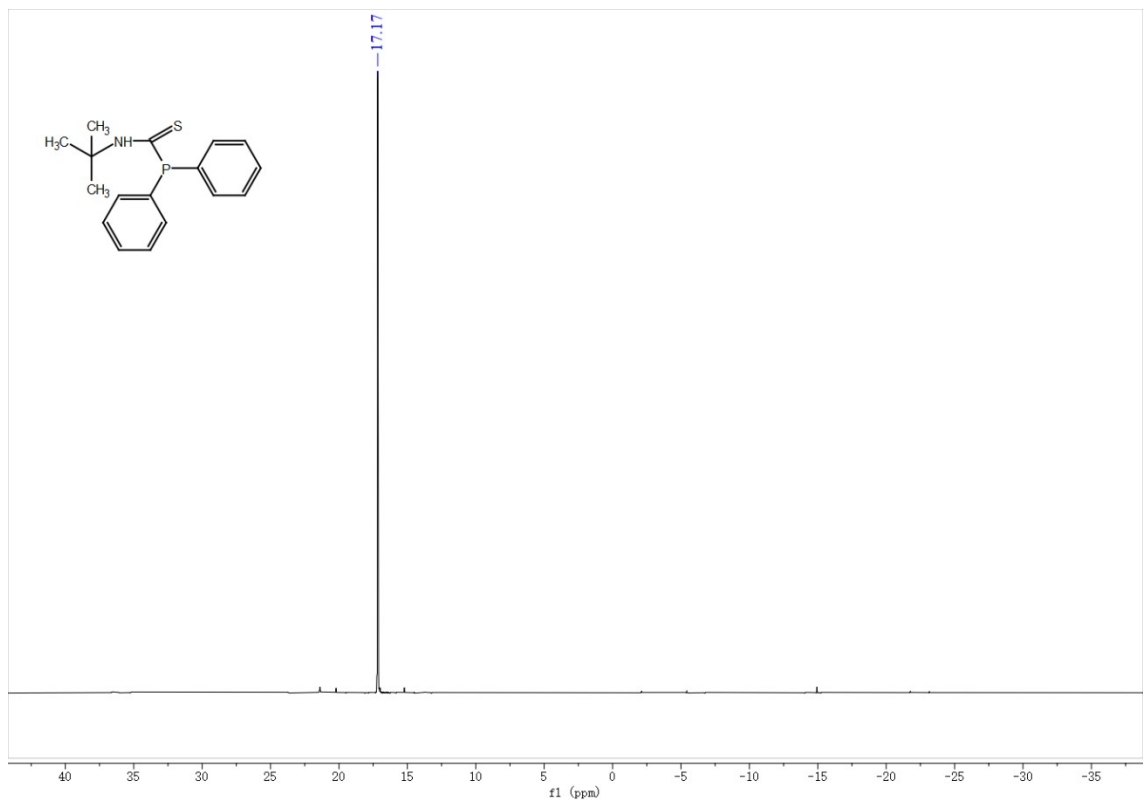
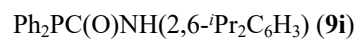


Figure S30. ^{31}P NMR spectrum (162 MHz, 298K, CDCl_3) of **9h**



White solid (99% yield). ^1H NMR (400 MHz, CDCl_3 , ppm) δ 7.68 – 7.54 (m, 4H, Ar-*H*), 7.36 – 7.32 (m, 6H, Ar-*H*), 7.21 – 7.12 (m, 1H, Ar-*H*), 7.08 – 6.98 (m, 2H, Ar-*H*), 6.79 – 6.54 (s, 1H, NH), 2.91 – 2.80 (m, 2H, $\text{CH}(\text{CH}_3)_2$), 1.07 – 1.01 (m, 12H, $\text{CH}(\text{CH}_3)_2$). ^{13}C NMR (101 MHz, CDCl_3 , ppm) δ 180.47 – 170.75 (d, *J* = 15.0 Hz), 147.71, 135.26 – 132.08 (d, *J* = 19.5 Hz), 132.62 – 132.19 (d, *J* = 10.8 Hz), 129.27, 128.27 – 127.16 (d, *J* = 7.5 Hz), 123.31, 30.00, 23.87. ^{31}P NMR (162 MHz, CDCl_3 , ppm) δ -3.27.

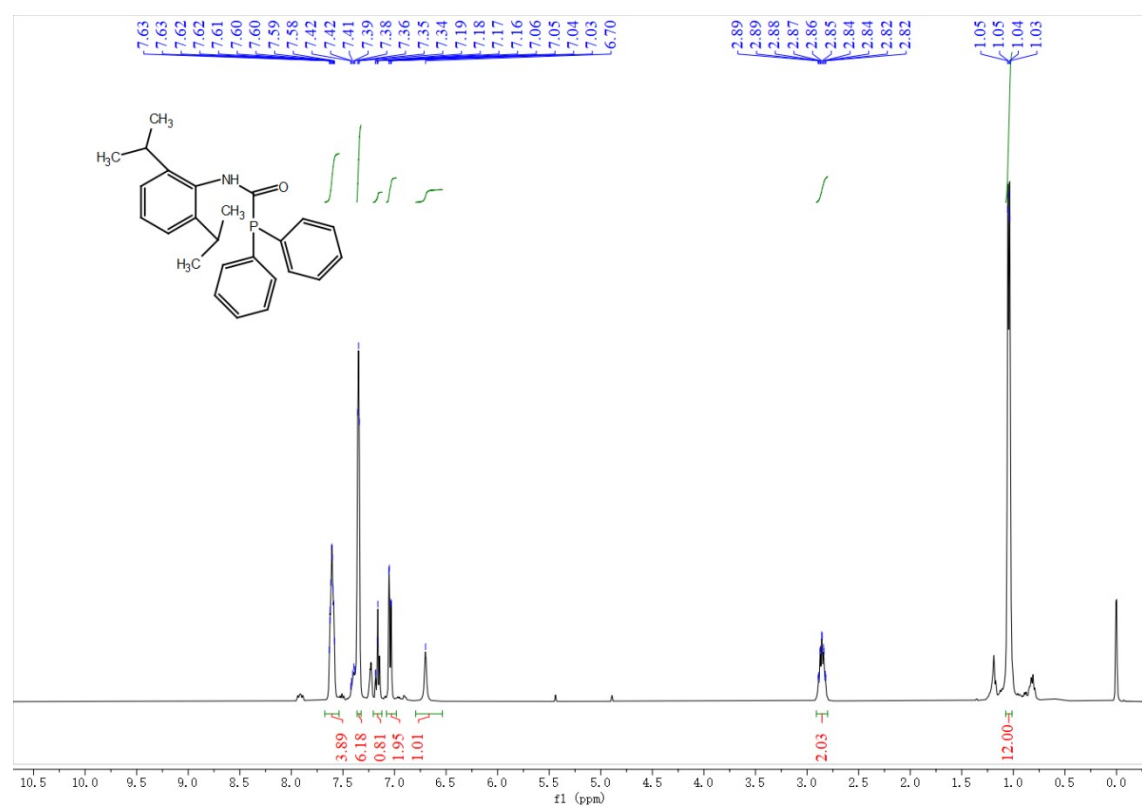


Figure S31. ^1H NMR spectrum (400 MHz, 298K, CDCl_3) of **9i**

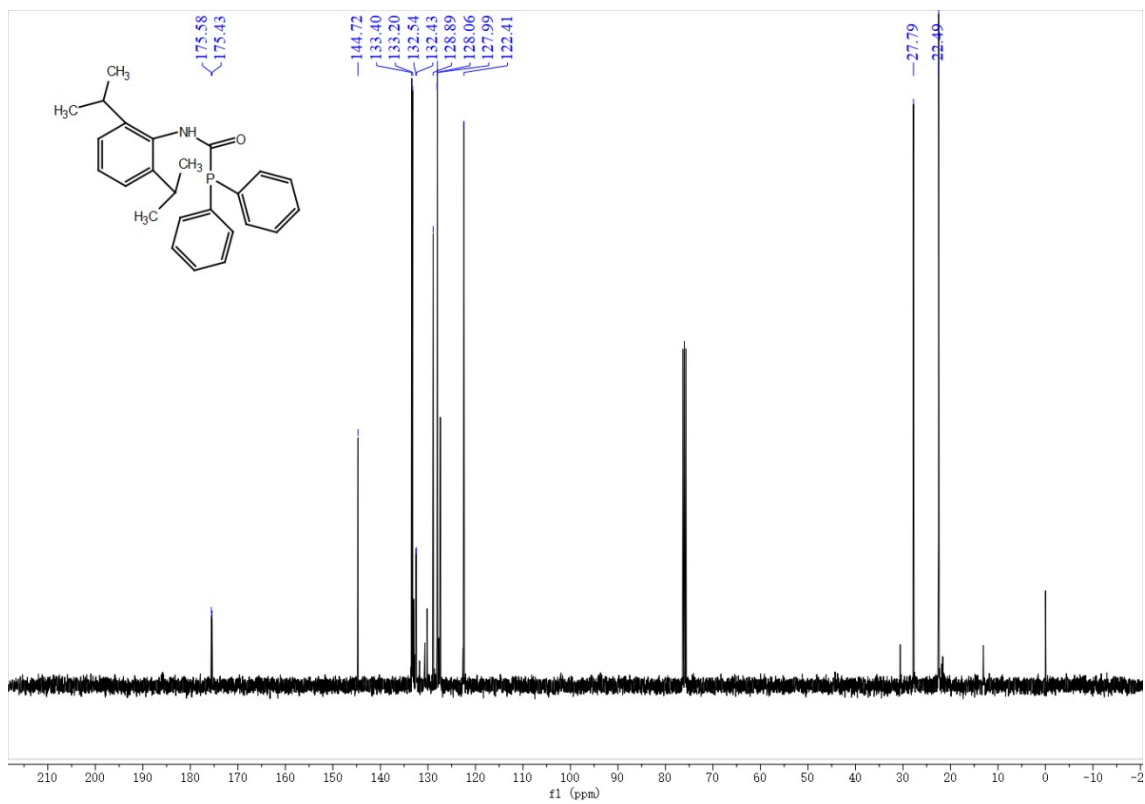


Figure S32. ^{13}C NMR spectrum (101 MHz, 298K, CDCl_3) of **9i**

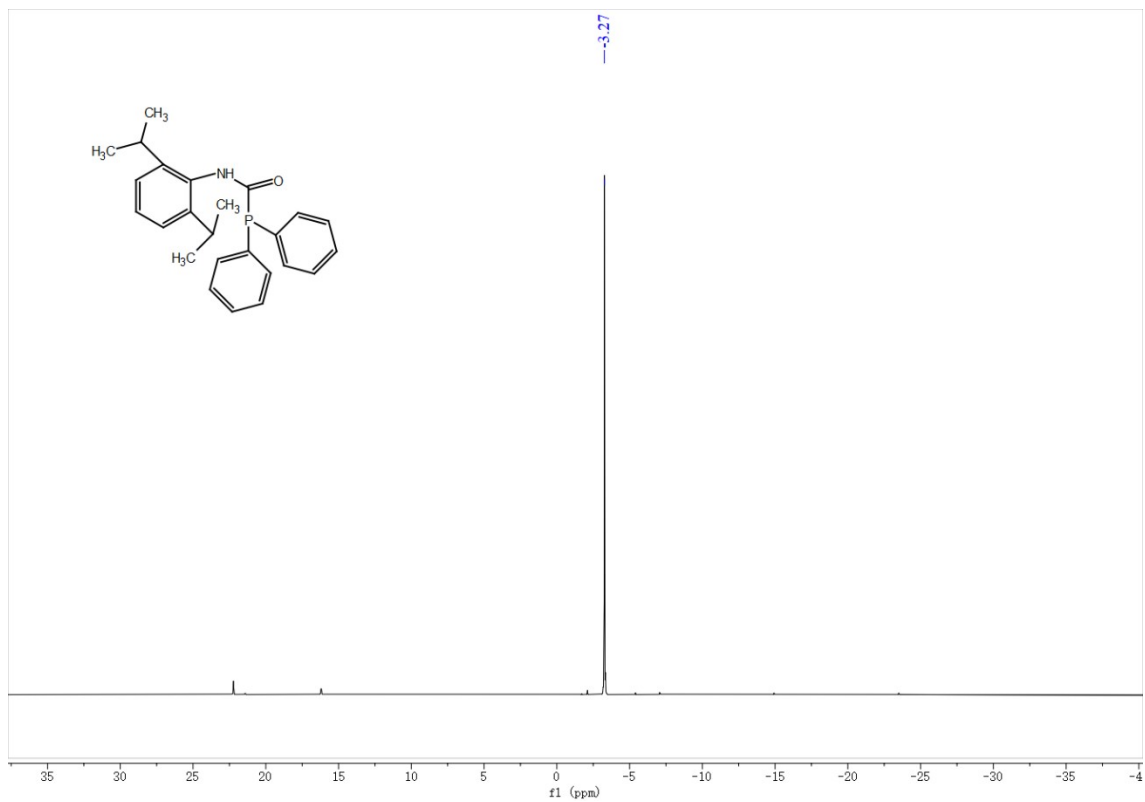


Figure S33. ^{31}P NMR spectrum (162 MHz, 298K, CDCl_3) of **9i**

$\text{Ph}_2\text{PC(O)NH(2,6-}^i\text{Pr}_2\text{C}_6\text{H}_3)$ (**9j**) and $\text{Ph}_2\text{PC(O)N(2,6-}^i\text{Pr}_2\text{C}_6\text{H}_3)\text{C(O)NH(2,6-}^i\text{Pr}_2\text{C}_6\text{H}_3)$ (**9k**)

The emergence of $\text{CH}(\text{CH}_3)_2$ signal of single insertion product **9j** at δ 1.24 – 1.13 ppm. Analogous, $\text{CH}(\text{CH}_3)_2$ signal of double insertion product **9k** emergences at δ 1.24 – 1.13 ppm and δ 0.97 – 0.90 ppm, and partially overlap with **6j** at δ 1.24 – 1.13 ppm. The ratio of the two products **9j** and **9k** can be obtained from the integration of the signal areas at the two locations.

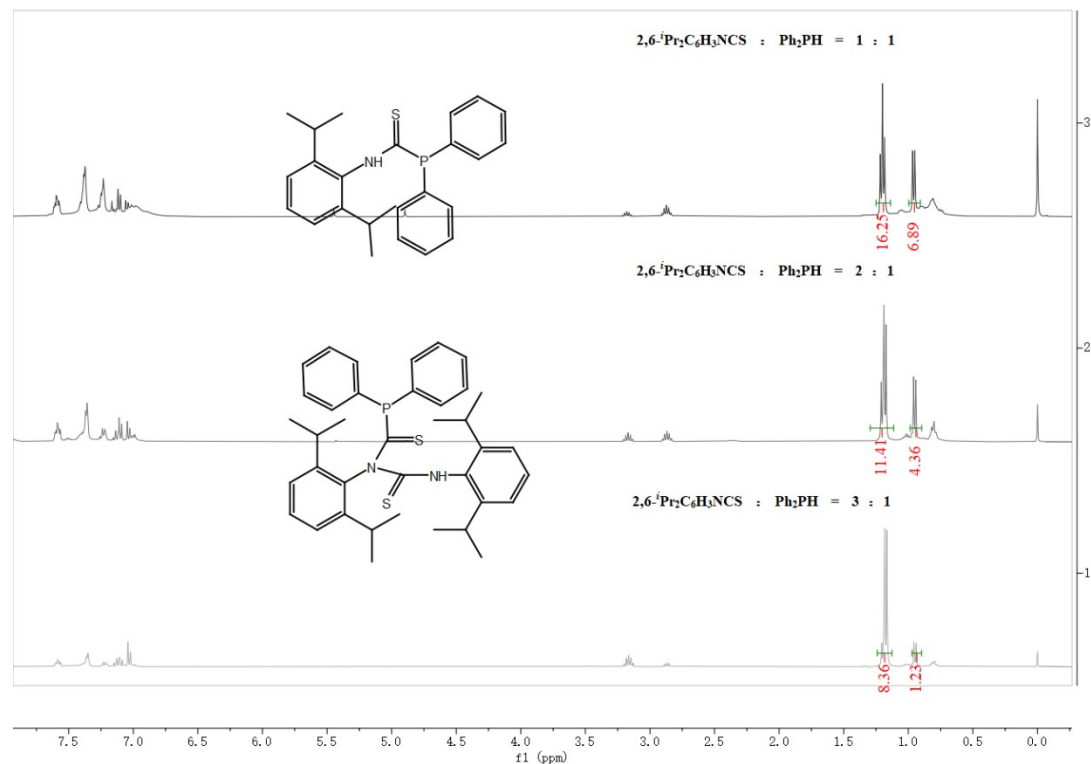


Figure S34. ^1H NMR spectrum (400 MHz, 298K, CDCl_3) of **9j** and **9k**

References

- [1] Z. Yang, M. Zhong, X. Ma, K. Nijesh, S. De, P. Parameswaran and H. W. Roesky, *J. Am. Chem. Soc.*, 2016, **138**, 2548-2551.
- [2] G. Feng, C. Du, L. Xiang, I. del Rosal, G. Li, X. Leng, E. Y. X. Chen, L. Maron and Y. Chen, *ACS Catal.*, 2018, **8**, 4710-4718.
- [3] W.-X. Zhang, M. Nishiura and Z. Hou, *Chem. Commun. (Cambridge, U. K.)*, 2006, **36**, 3812-3814.
- [4] M. R. Crimmin, A. G. M. Barrett, M. S. Hill, P. B. Hitchcock and P. A. Procopiou, *Organometallics*, 2008, **27**, 497-499.
- [5] A. C. Behrle and J. A. R. Schmidt, *Organometallics*, 2013, **32**, 1141-1149.
- [6] X. Gu, L. Zhang, X. Zhu, S. Wang, S. Zhou, Y. Wei, G. Zhang, X. Mu, Z. Huang, D. Hong and F. Zhang, *Organometallics*, 2015, **34**, 4553-4559.
- [7] A. Martinez, S. Moreno-Blazquez, A. Rodriguez-Dieguez, A. Ramos, R. Fernandez-Galan, A. Antinolo and F. Carrillo-Hermosilla, *Dalton Trans.*, 2017, **46**, 12923-12934.
- [8] T. M. Horsley Downie, J. W. Hall, T. P. Collier Finn, D. J. Liptrot, J. P. Lowe, M. F. Mahon, C. L. McMullin and M. K. Whittlesey, *Chem. Commun. (Cambridge, U. K.)*, 2020, **56**, 13359-13362.
- [9] M. Itazaki, T. Matsutani, T. Nochida, T. Moriuchi and H. Nakazawa, *Chem. Commun. (Cambridge, U. K.)*, 2020, **56**, 443-445.
- [10] J. G. Noltes, *Recueil Des Travaux Chimiques Des Pays-Bas*, 1965, **84**, 782-&.

[11] G. M. Sheldrick SADABS, University of Göttingen, Germany, 1997, **28**, 53-56.

[12] G. Sheldrick, *Acta Crystallogr. A*, 2015, **71**, 3-8.

[13] G. Sheldrick, *Acta Crystallogr. C*, 2015, **71**, 3-8.